Lecture 3 Cross Section Measurements

Ingredients to a Cross Section

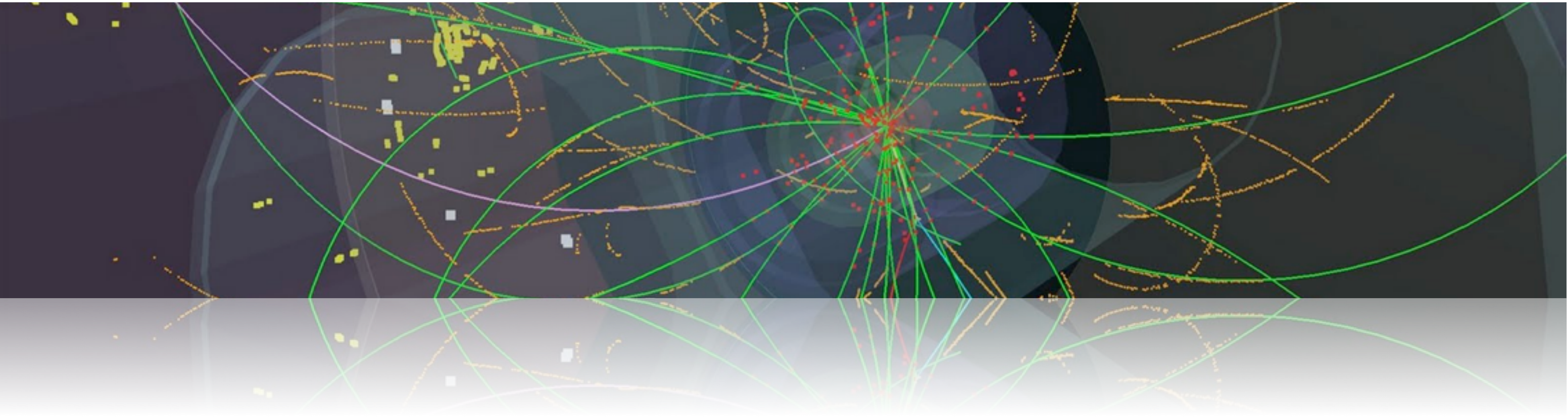

Prerequisites and Reminders ...

Natural Units
Four-Vector Kinematics
Lorentz Transformation
Lorentz Boost
Lorentz Invariance
Rapidity etc.
Invariant Mass
CMS-Energy

Particle Decays
Cross Section
Matrix Element
Phase Space
Feynman Diagrams
Mandelstam Variables

Parton Distributions
Bjorken-x
...

$$\hbar = 1,\ c = 1$$

$$\hbar c = 197.3 \text{ MeV fm}$$
$$(\hbar c)^2 = 0.3894 \text{ GeV}^2 \text{ mb}$$

$$p = (E, \vec{p}\,)$$

$$p^2 = E^2 - \vec{p}^{\,2} = m^2$$

$$\beta = p/E,\ \gamma = E/m$$

$$p_1 \cdot p_2 = E_1 E_2 - \vec{p}_1 \cdot \vec{p}_2$$

4-vector scalar product
Lorentz invariant

→ All quantities like cross sections etc.
should be in terms of scalar products of 4-vectors ...

Prerequisites and Reminders ...

Natural Units
Four-Vector Kinematics
Lorentz Transformation
Lorentz Boost
Lorentz Invariance
Rapidity etc.
Invariant Mass
CMS-Energy

Particle Decays
Cross Section
Matrix Element
Phase Space
Feynman Diagrams
Mandelstam Variables

Parton Distributions
Bjorken-x
...

$$p = (E, \vec{p}\,)$$

Particle momentum as seen
in laboratory frame ...

$$p^* = (E^*, \vec{p}^{\,*})$$

Particle momentum as viewed from a
frame moving with velocity β_f ...

Lorentz Transformation:

$$E^* = \gamma_f \cdot E - \gamma_f \beta_f \cdot p_{||}$$
$$p_{||}^* = \gamma_f \cdot p_{||} - \gamma_f \beta_f \cdot E$$
$$p_T^* = p_T$$

with $\gamma_f = (1 - \beta_f^2)^{-\frac{1}{2}}$

Prerequisites and Reminders ...

Natural Units
Four-Vector Kinematics
Lorentz Transformation
Lorentz Boost
Lorentz Invariance
Rapidity etc.
Invariant Mass
CMS-Energy

Particle Decays
Cross Section
Matrix Element
Phase Space
Feynman Diagrams
Mandelstam Variables

Parton Distributions
Bjorken-x
...

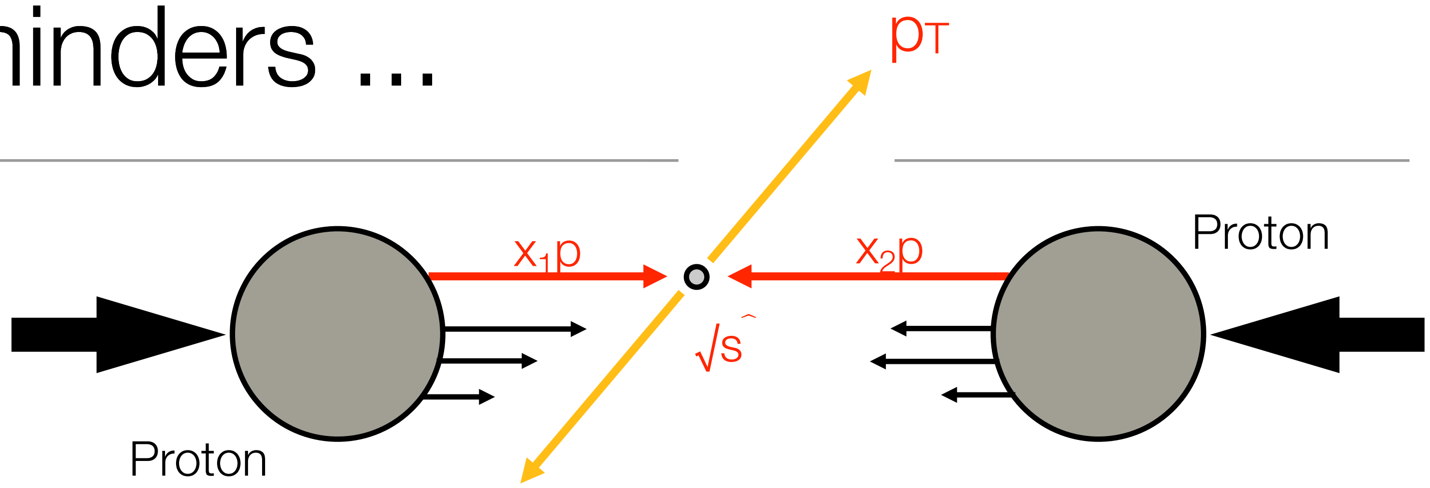

Schematic
proton-proton scattering

Relevant kinematic variables:

- Transverse momentum: p_T
- Rapidity: $y = ½\cdot\ln (E-p_z)/(E+p_z)$
- Pseudorapidity: $\eta = -\ln \tan ½\theta$
- Azimuthal angle: ϕ

Pseudorapidity

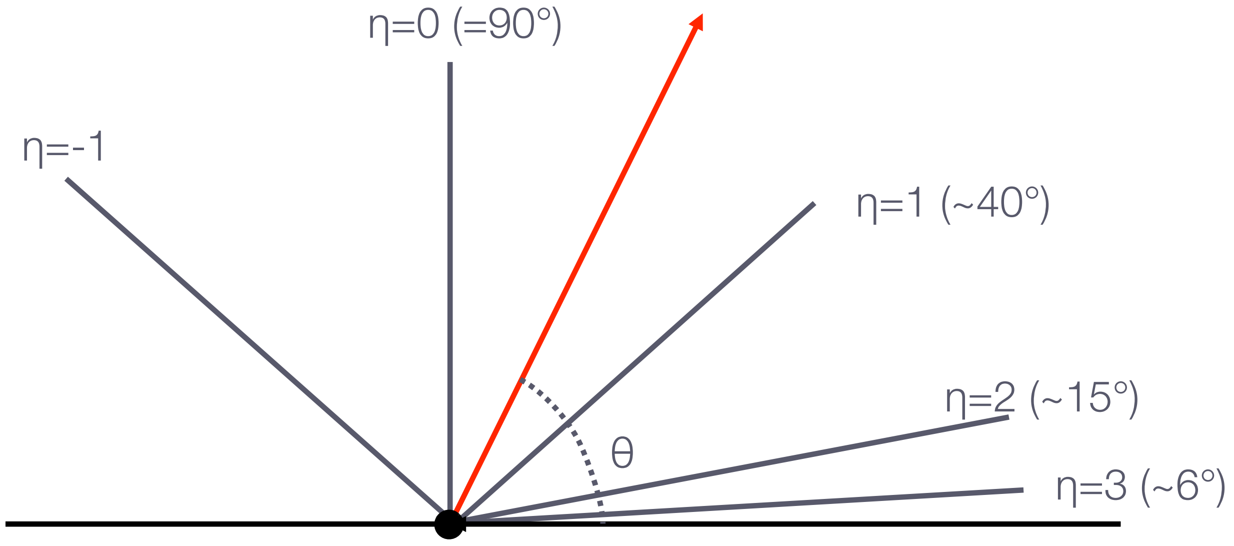

Prerequisites and Reminders ...

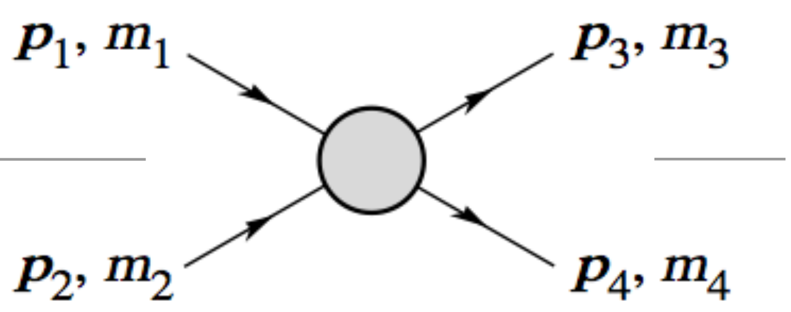

Natural Units
Four-Vector Kinematics
Lorentz Transformation
Lorentz Boost
Lorentz Invariance
Rapidity etc.
Invariant Mass
CMS-Energy

Particle Decays
Cross Section
Matrix Element
Phase Space
Feynman Diagrams
Mandelstam Variables

Parton Distributions
Bjorken-x
...

Invariant Mass:

$$M^2 = (p_1 + p_2)^2$$
$$= (E_1 + E_2)^2 - (\vec{p}_1 + \vec{p}_2)^2$$
$$= m_1^2 + m_2^2 + 2E_1E_2(1 - \vec{\beta}_1\vec{\beta}_2)$$

Center-of-mass Energy:

$$E_{\mathrm{cm}} = \left[(E_1 + E_2)^2 - (\vec{p}_1 + \vec{p}_2)^2\right]^{\frac{1}{2}}$$

Particle 2 at rest:

$$E_{\mathrm{cm}} = \left[m_1^2 + m_2^2 + 2E_1m_2\right]^{\frac{1}{2}}$$

Particle Collider:

$[E_1 = E_2;\ \vec{p}_1 = -\vec{p}_2;\ m_1 = m_2 \approx 0]$

$$E_{\mathrm{cm}} = 2E$$

Prerequisites and Reminders ...

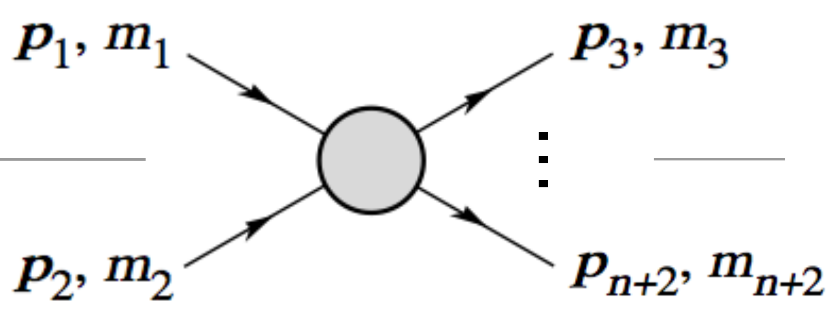

Natural Units
Four-Vector Kinematics
Lorentz Transformation
Lorentz Boost
Lorentz Invariance
Rapidity etc.
Invariant Mass
CMS-Energy

Cross Section
Particle Decays
Matrix Element
Phase Space
Feynman Diagrams
Mandelstam Variables

Parton Distributions
Bjorken-x
...

Differential Cross Section:

Matrix element

$$d\sigma = \frac{(2\pi)^4 |\mathcal{M}|^2}{4\sqrt{(p_1 \cdot p_2)^2 - m_1^2 m_2^2}} \times d\Phi_n(p_1 + p_2;\ p_3, \ldots, p_{n+2})$$

n-body phase space

$$d\Phi_n = \ldots$$

$$\ldots = \delta^4\left(P - \sum_{i=1}^{n} p_i\right) \prod_{i=1}^{n} \frac{d^3 p_i}{(2\pi)^3 2E_i}$$

with $P = p_1 + p_2$

Partial Decay Rate:

$$d\Gamma = \frac{(2\pi)^4}{2M} |\mathcal{M}|^2 \times d\Phi_n(P;\ p_1, \ldots, p_n)$$

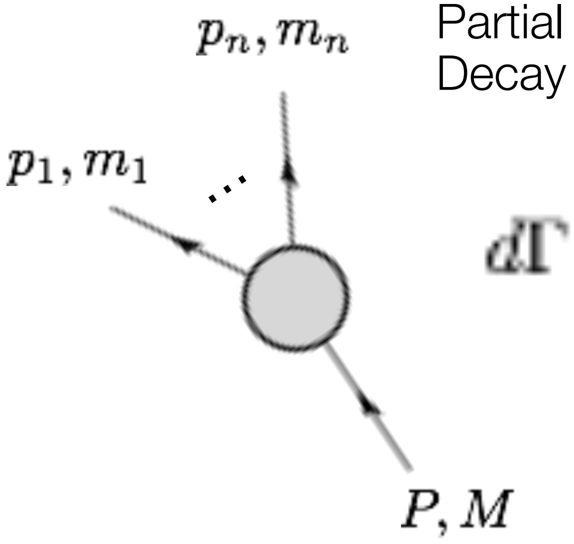

Prerequisites and Reminders ...

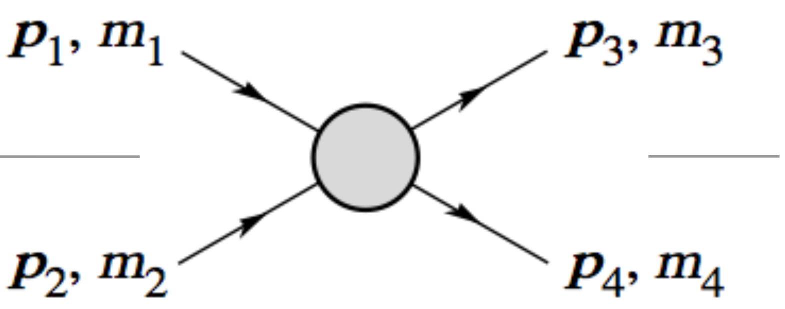

Natural Units
Four-Vector Kinematics
Lorentz Transformation
Lorentz Boost
Lorentz Invariance
Rapidity etc.
Invariant Mass
CMS-Energy

Particle Decays
Cross Section
Matrix Element
Phase Space
Feynman Diagrams
Mandelstam Variables

Parton Distributions
Bjorken-x
...

Mandelstam variables:

$$s = (p_1 + p_2)^2 = (p_3 + p_4)^2$$
$$t = (p_1 - p_3)^2 = (p_2 - p_4)^2$$
$$u = (p_1 - p_4)^2 = (p_2 - p_3)^2$$

s-channel

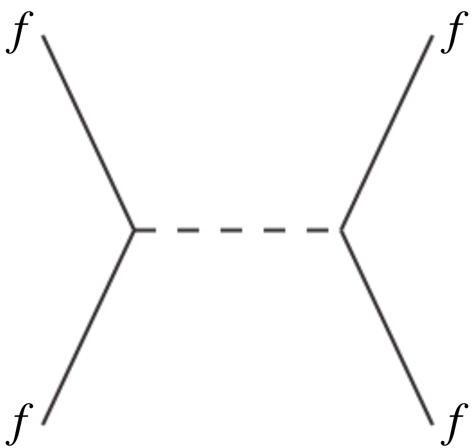

$$\sigma \propto \frac{t^2 + u^2}{s^2}$$

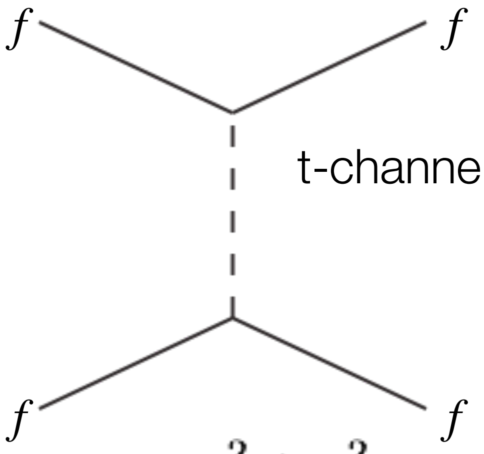

t-channel

$$\sigma \propto \frac{s^2 + u^2}{t^2}$$

u-channel

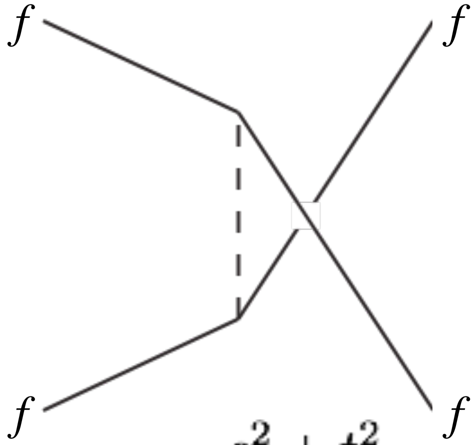

$$\sigma \propto \frac{s^2 + t^2}{u^2}$$

Prerequisites and Reminders ...

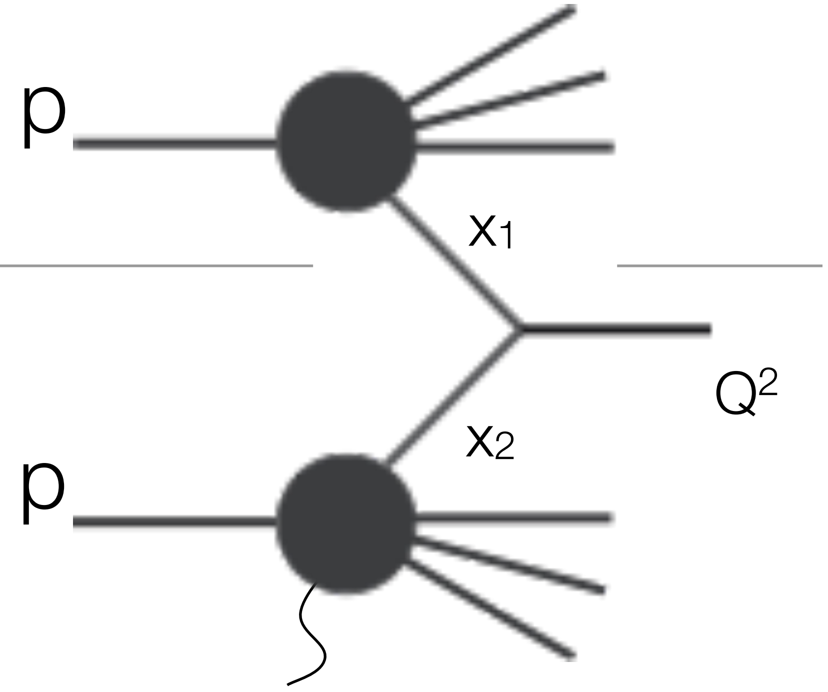

Natural Units
Four-Vector Kinematics
Lorentz Transformation
Lorentz Boost
Lorentz Invariance
Rapidity etc.
Invariant Mass
CMS-Energy

Particle Decays
Cross Section
Matrix Element
Phase Space
Feynman Diagrams
Mandelstam Variables

Parton Distributions
Bjorken-x
...

Proton-Proton
Cross Section:

$$\sigma = \sum_{ij} \int dx_1 dx_2 \; f_i(x_1, Q^2) \, f_j(x, Q^2) \; \hat{\sigma}(Q^2)$$

Parton content:
$f(x,Q^2) = q(x,Q^2)$ or $g(x,Q^2)$

$x_{1,2}$: Bjorken-x
fractional momentum of parton
involve in hard process

Q^2 : scale; spatial resolution
invariant parton-parton mass

f : Parton Distribution function
measured e.g. at HERA ...

Proton-Proton Scattering @ LHC

- Hard interaction: qq, gg, qg fusion
- Initial State Radiation (ISR)
- Secondary Interaction
  ["underlying event"]

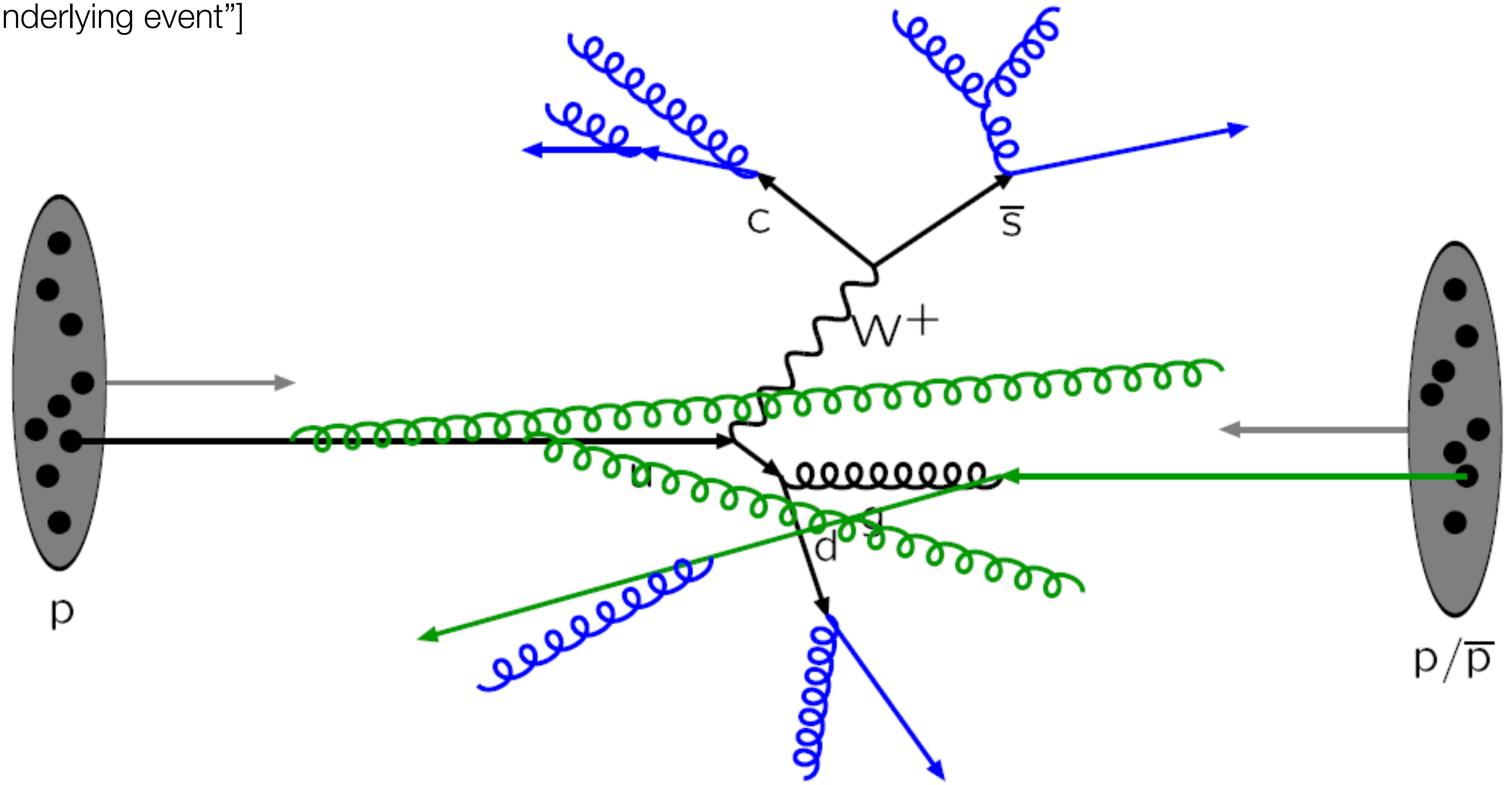

Proton-Proton Scattering @ LHC

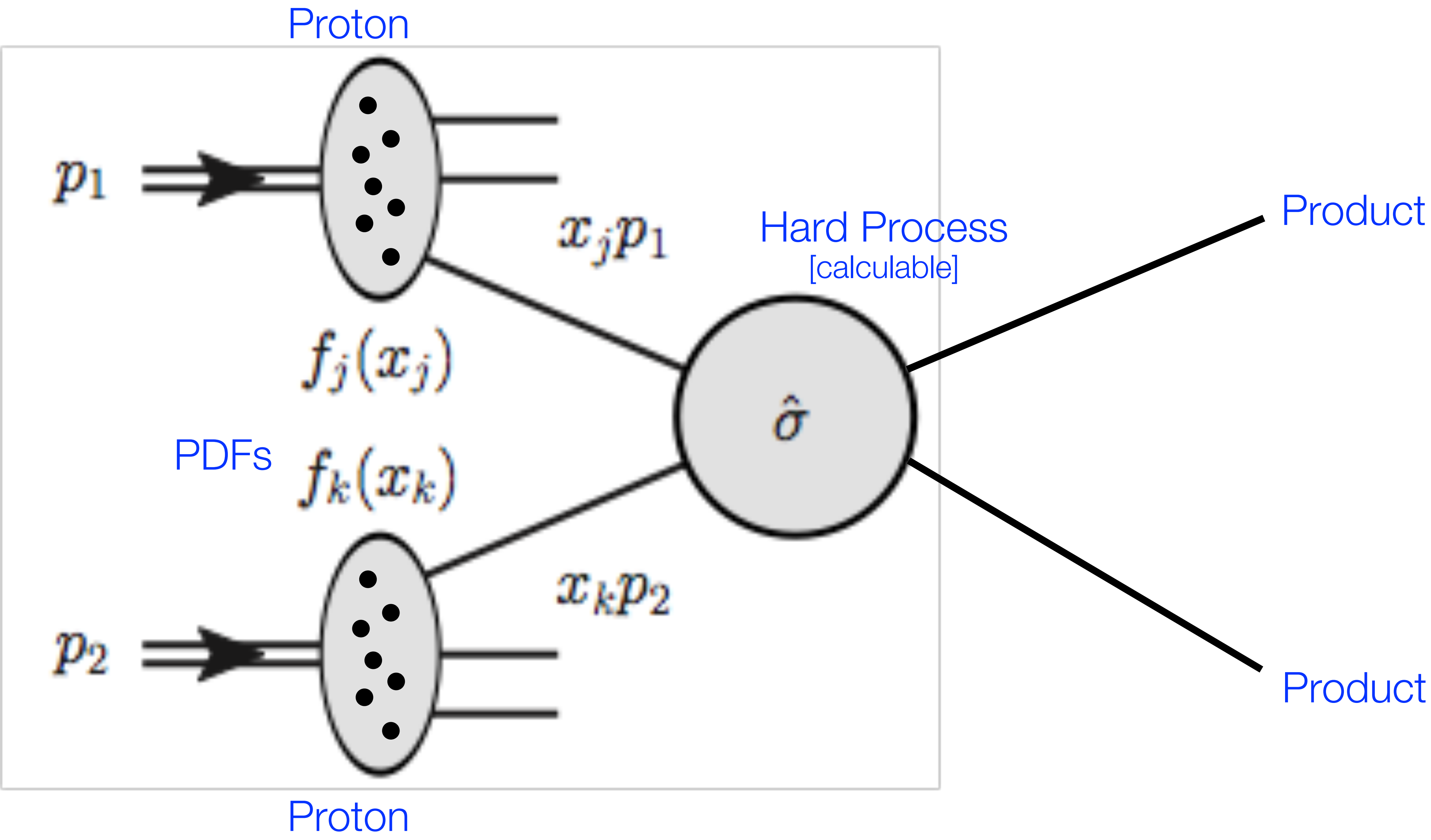

Some Hard Processes ...

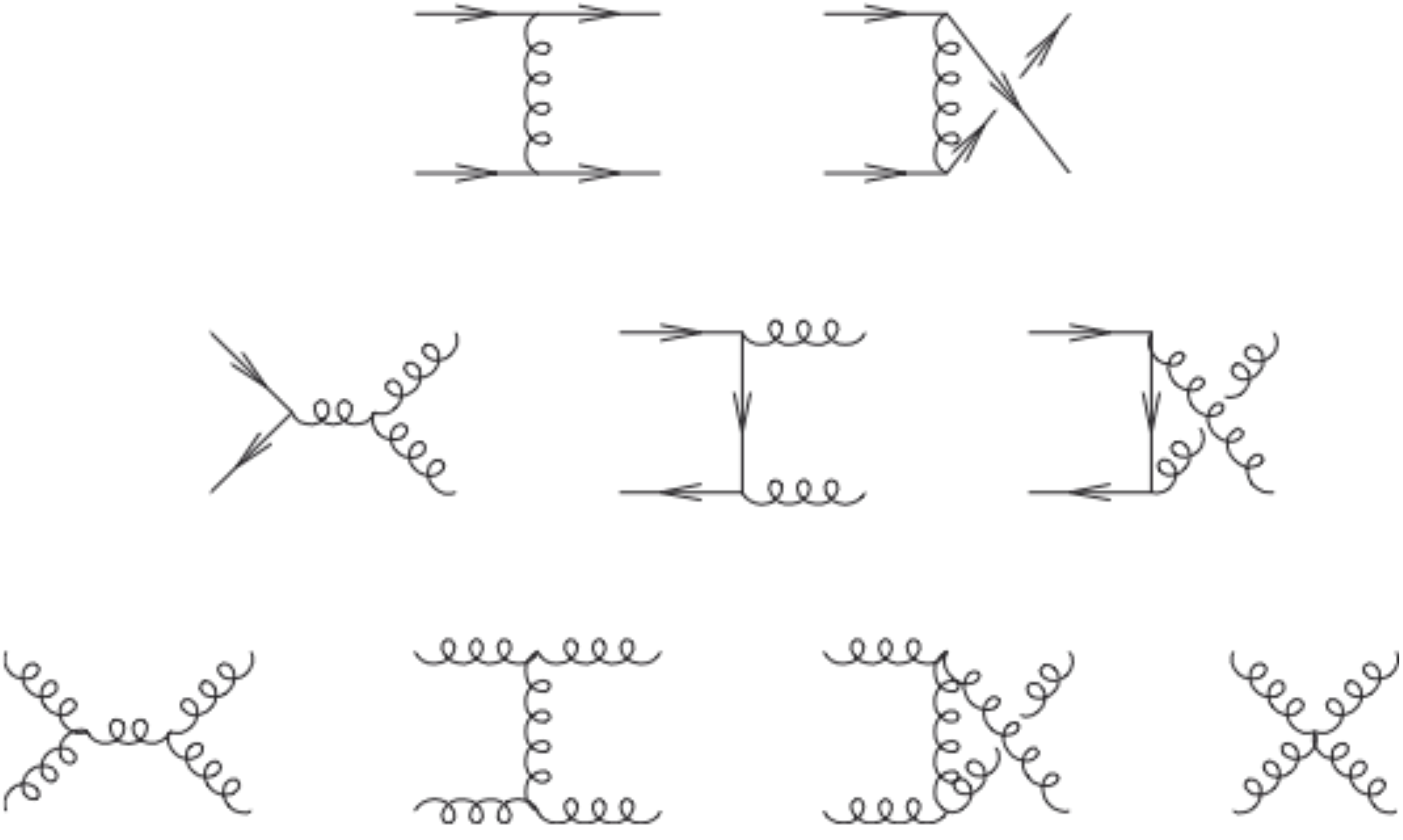

QCD Matrix Elements

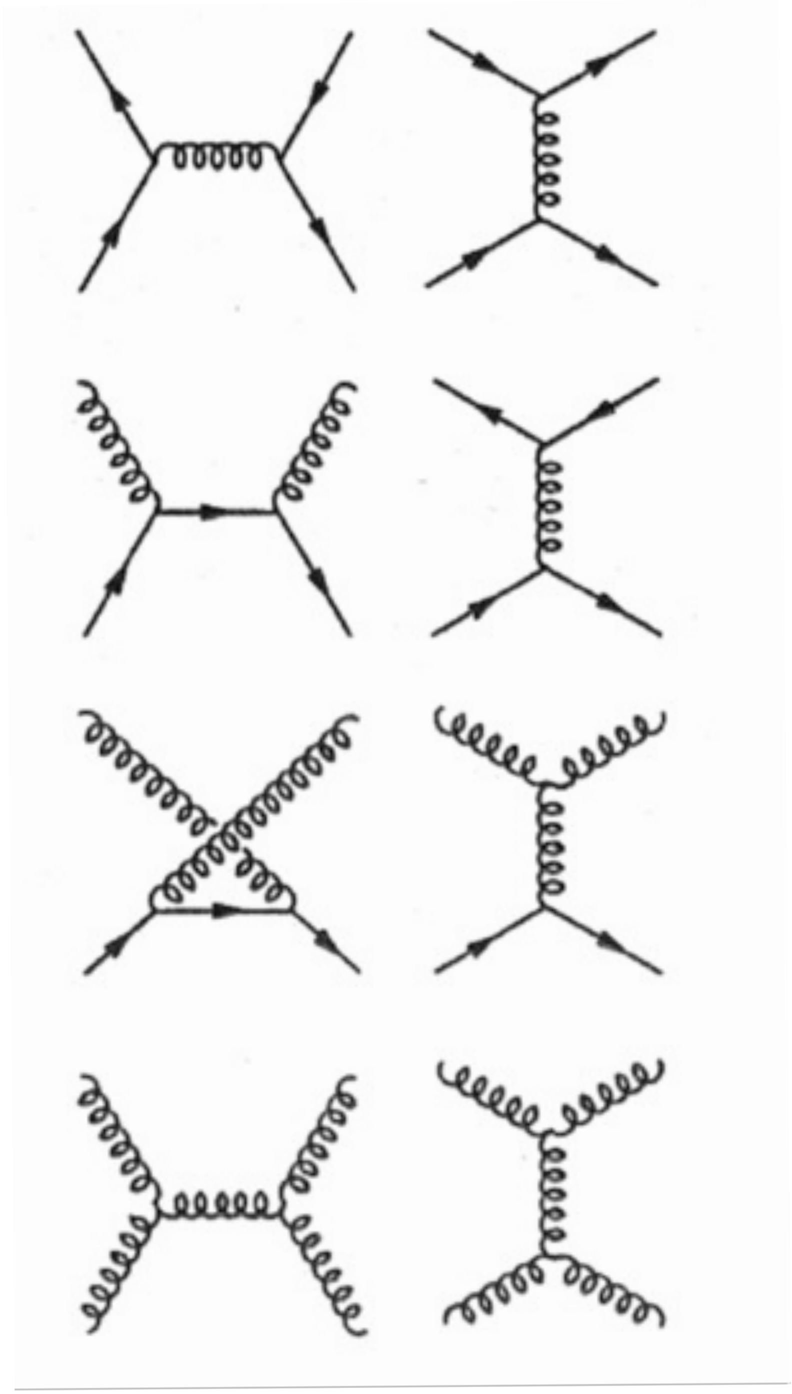

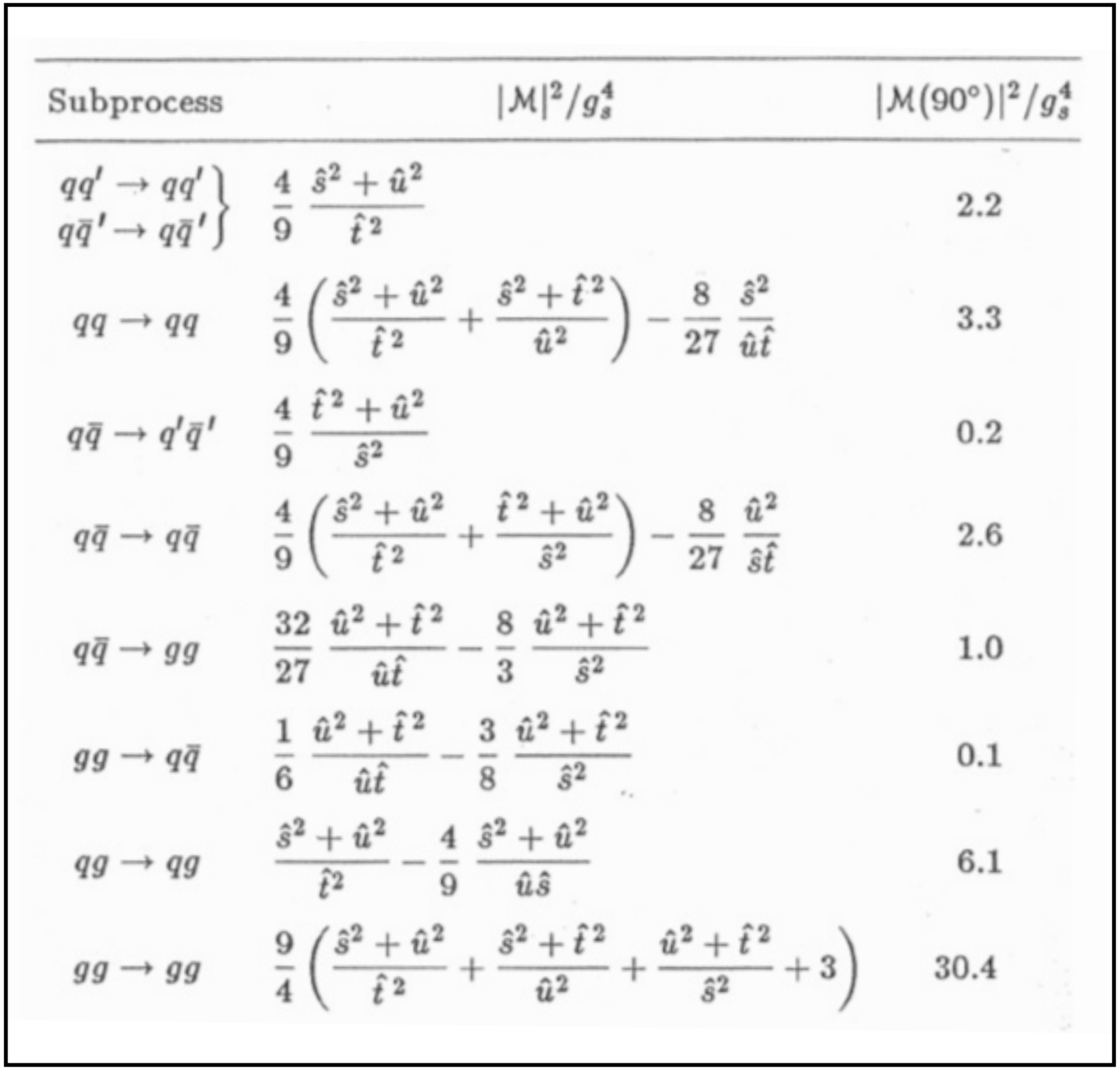

Subprocess	$\|\mathcal{M}\|^2/g_s^4$	$\|\mathcal{M}(90^\circ)\|^2/g_s^4$
$\left.\begin{matrix} qq' \to qq' \\ q\bar{q}' \to q\bar{q}' \end{matrix}\right\}$	$\frac{4}{9}\,\frac{\hat{s}^2+\hat{u}^2}{\hat{t}^2}$	2.2
$qq \to qq$	$\frac{4}{9}\left(\frac{\hat{s}^2+\hat{u}^2}{\hat{t}^2}+\frac{\hat{s}^2+\hat{t}^2}{\hat{u}^2}\right)-\frac{8}{27}\,\frac{\hat{s}^2}{\hat{u}\hat{t}}$	3.3
$q\bar{q} \to q'\bar{q}'$	$\frac{4}{9}\,\frac{\hat{t}^2+\hat{u}^2}{\hat{s}^2}$	0.2
$q\bar{q} \to q\bar{q}$	$\frac{4}{9}\left(\frac{\hat{s}^2+\hat{u}^2}{\hat{t}^2}+\frac{\hat{t}^2+\hat{u}^2}{\hat{s}^2}\right)-\frac{8}{27}\,\frac{\hat{u}^2}{\hat{s}\hat{t}}$	2.6
$q\bar{q} \to gg$	$\frac{32}{27}\,\frac{\hat{u}^2+\hat{t}^2}{\hat{u}\hat{t}}-\frac{8}{3}\,\frac{\hat{u}^2+\hat{t}^2}{\hat{s}^2}$	1.0
$gg \to q\bar{q}$	$\frac{1}{6}\,\frac{\hat{u}^2+\hat{t}^2}{\hat{u}\hat{t}}-\frac{3}{8}\,\frac{\hat{u}^2+\hat{t}^2}{\hat{s}^2}$	0.1
$qg \to qg$	$\frac{\hat{s}^2+\hat{u}^2}{\hat{t}^2}-\frac{4}{9}\,\frac{\hat{s}^2+\hat{u}^2}{\hat{u}\hat{s}}$	6.1
$gg \to gg$	$\frac{9}{4}\left(\frac{\hat{s}^2+\hat{u}^2}{\hat{t}^2}+\frac{\hat{s}^2+\hat{t}^2}{\hat{u}^2}+\frac{\hat{u}^2+\hat{t}^2}{\hat{s}^2}+3\right)$	30.4

Proton-Proton Scattering @ LHC

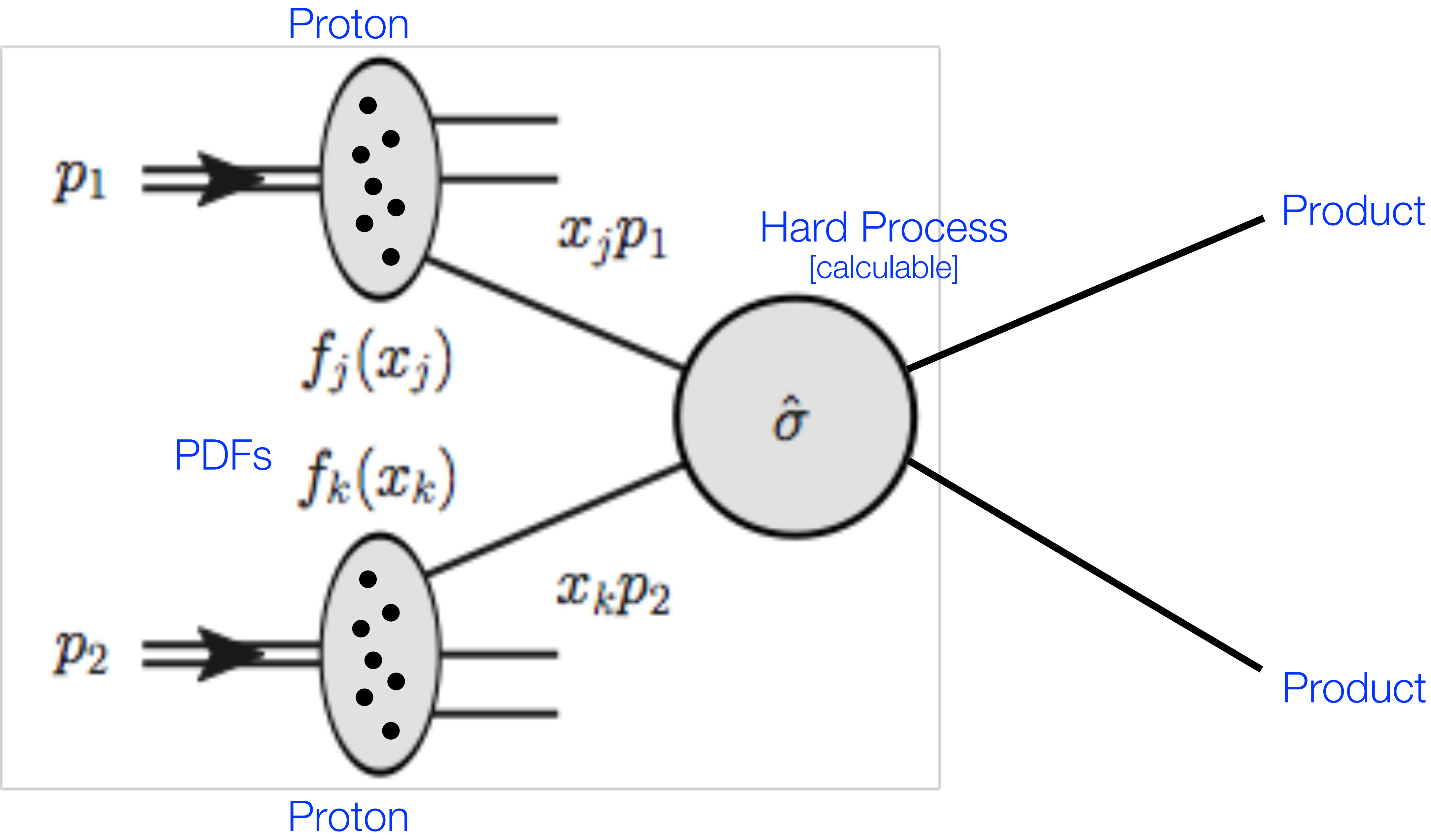

Electron-Proton Scattering @ HERA

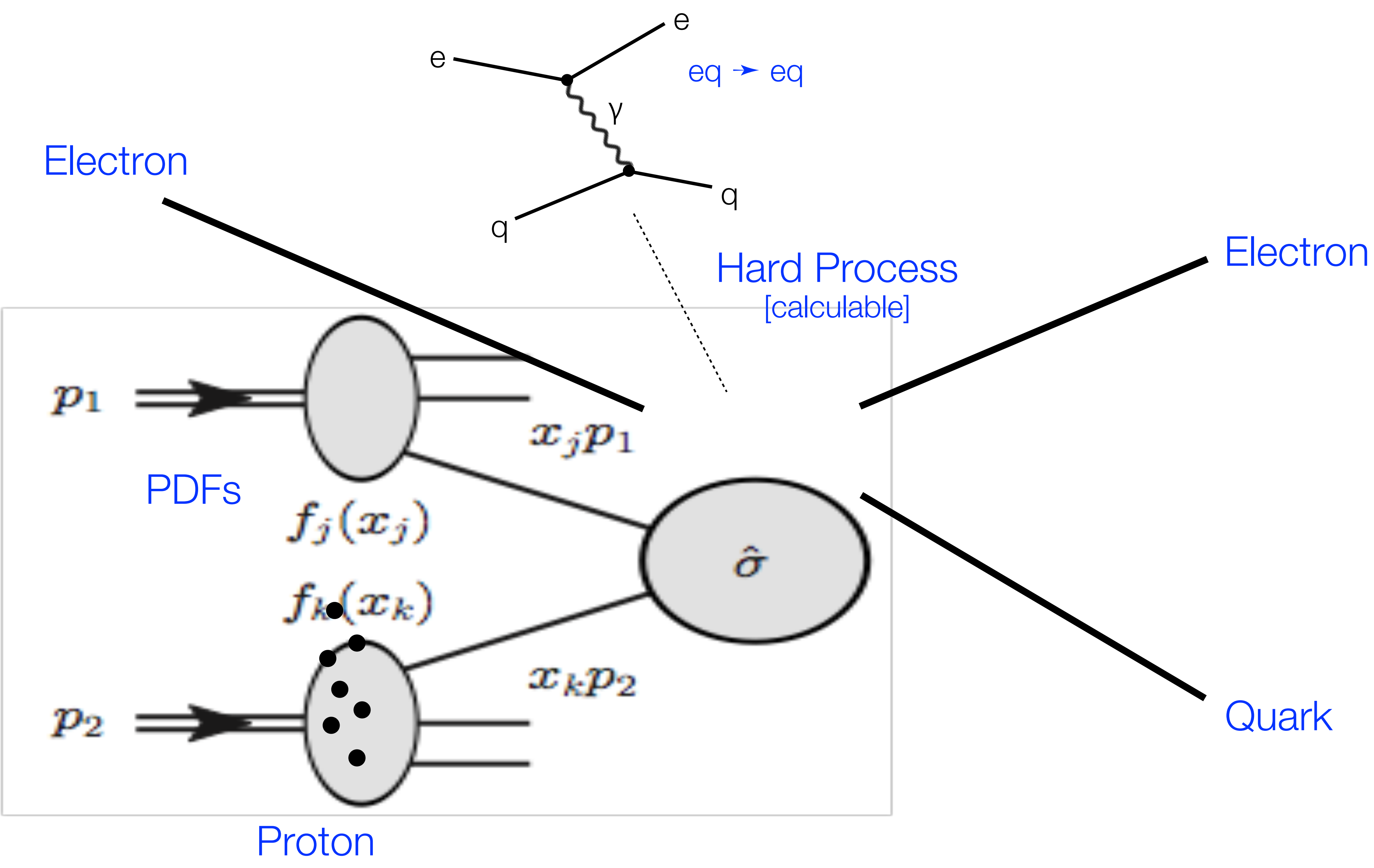

Electron-Proton Scattering @ HERA

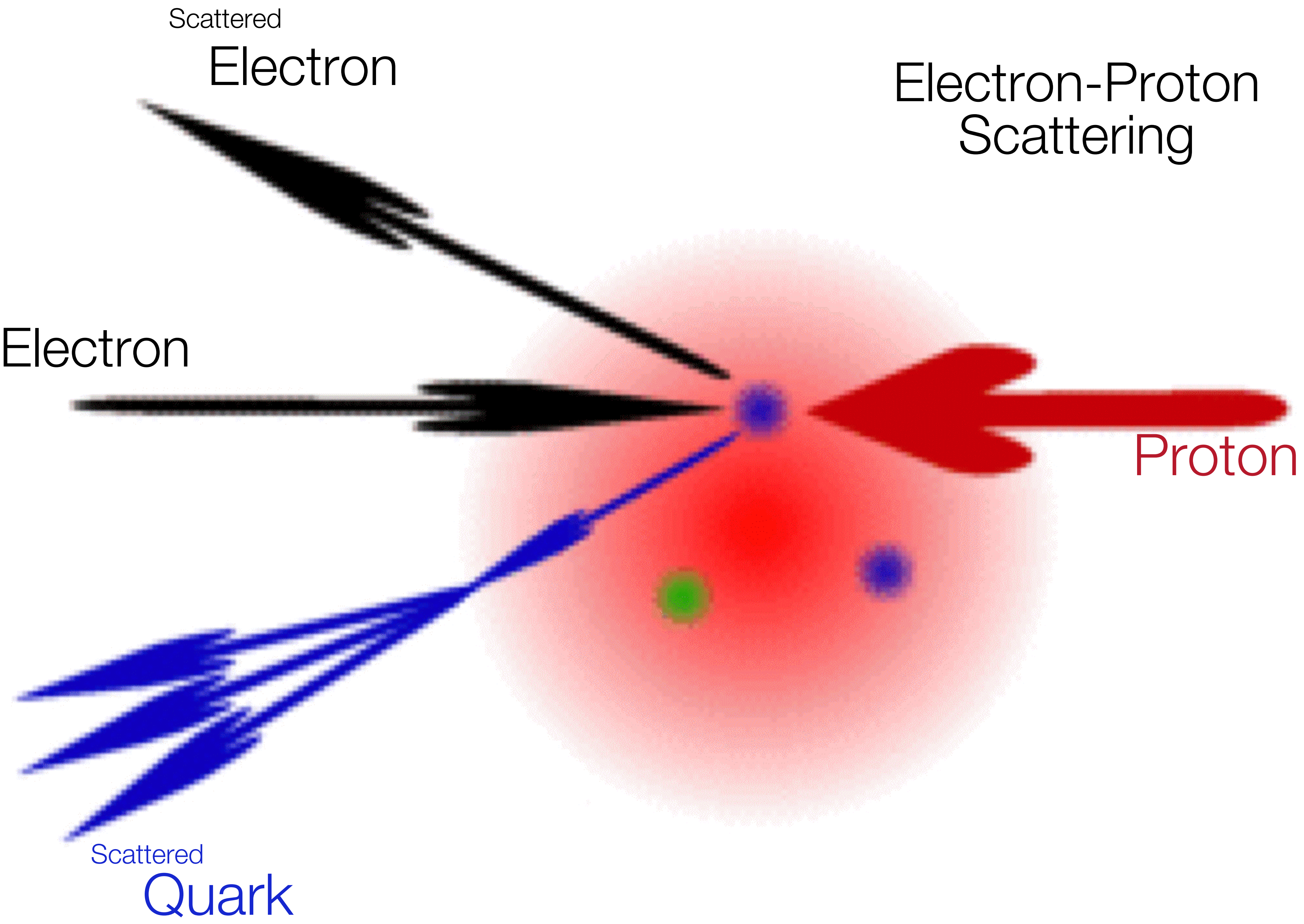

Electron-Proton Scattering @ HERA

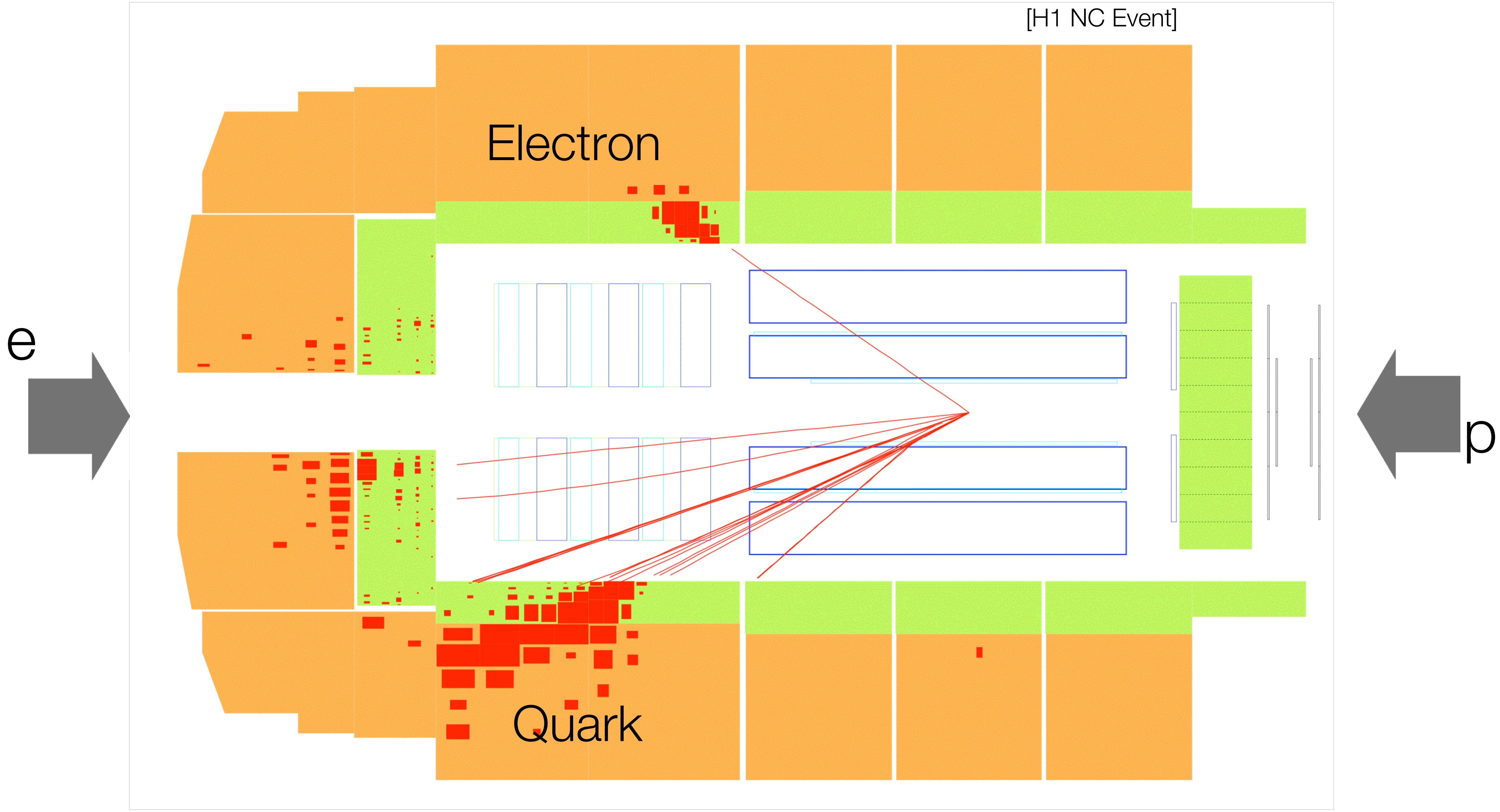

Electron-Proton Scattering @ HERA

E_e=27.5 GeV

Q^2: neg. four momentum transfer squared

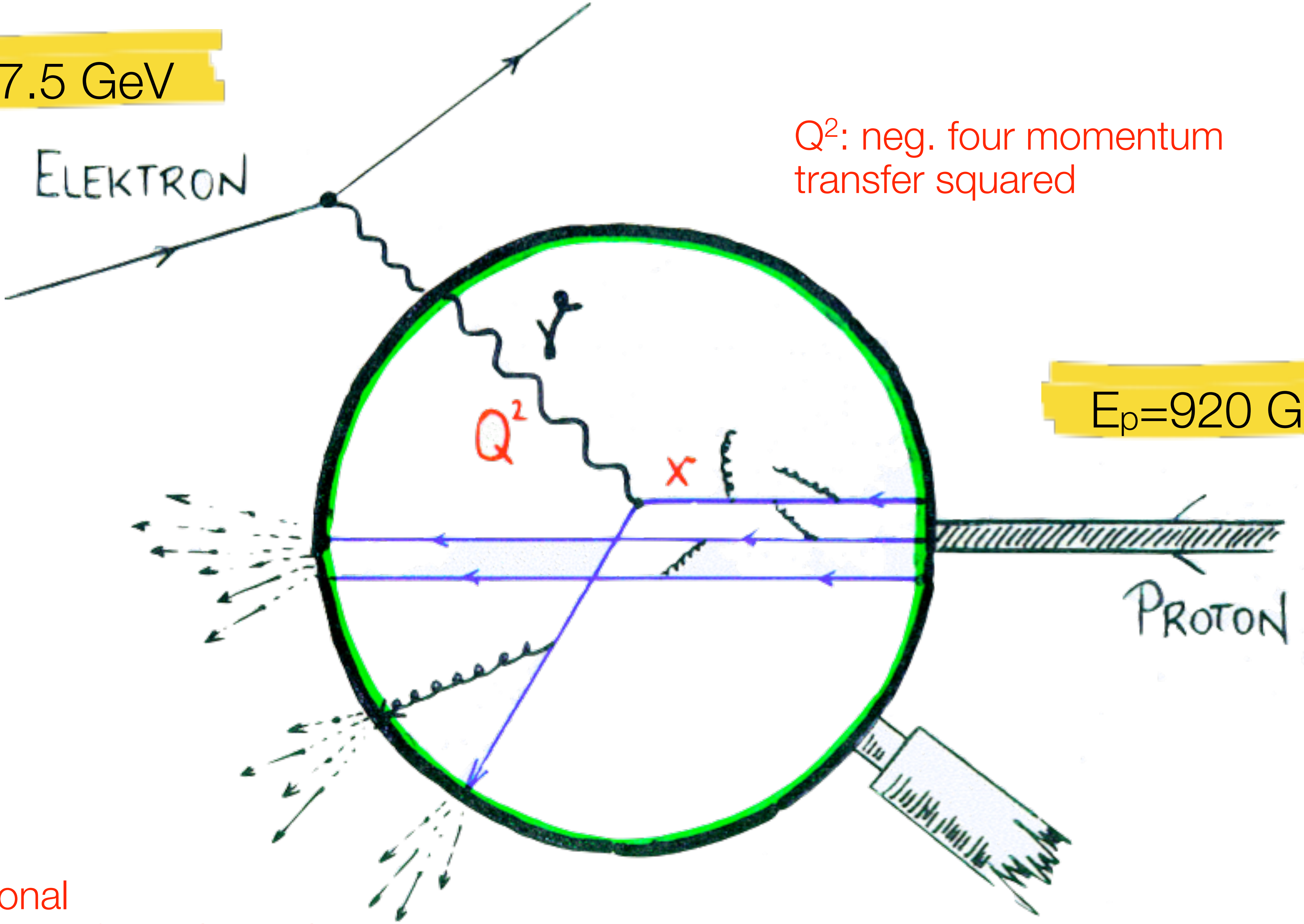

E_p=920 GeV

x : fractional momentum of struck quark

Electron-Proton Scattering @ HERA

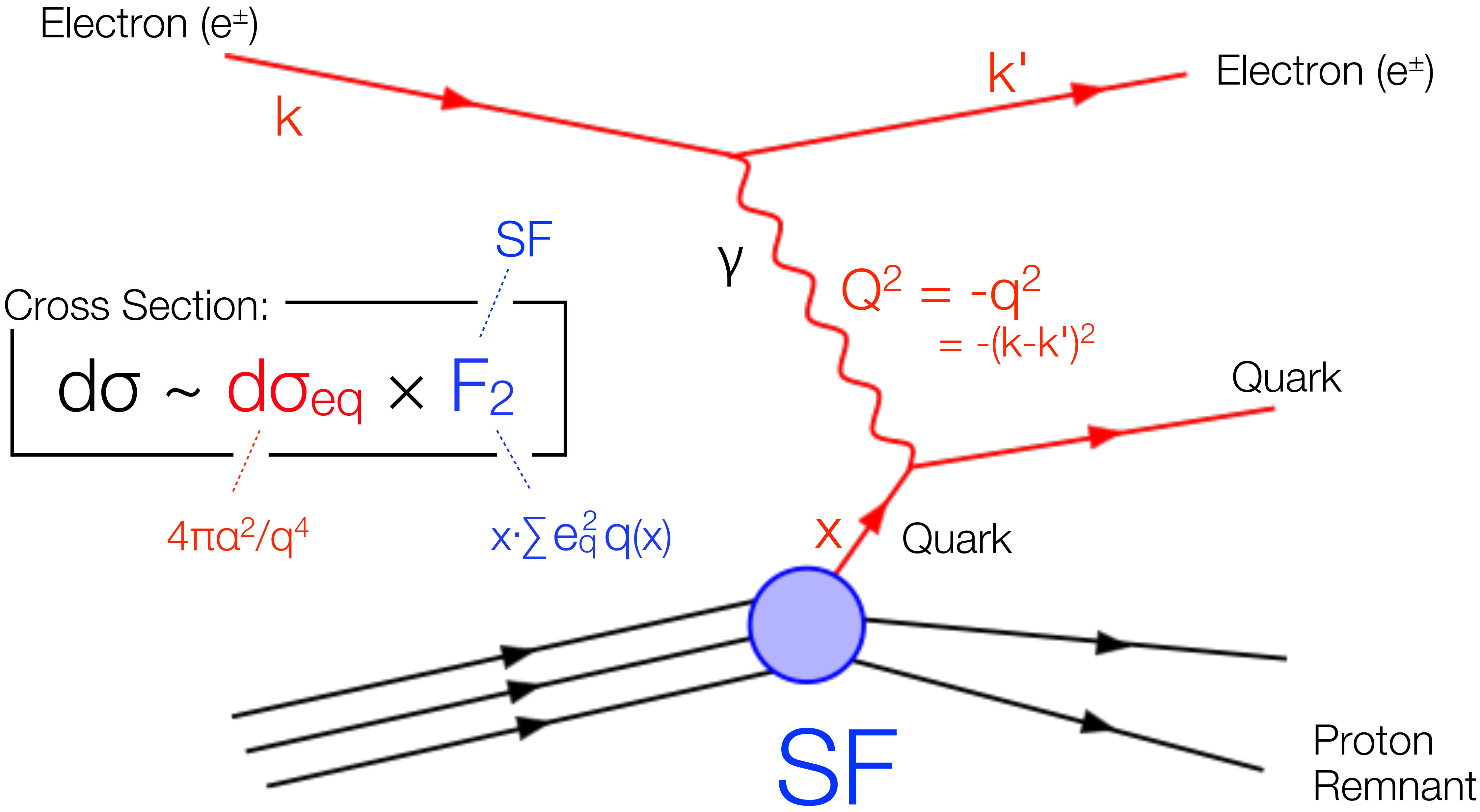

Cross Section:

$$d\sigma \sim \underbrace{d\sigma_{eq}}_{4\pi\alpha^2/q^4} \times \overset{SF}{\underbrace{F_2}_{x\cdot\sum e_q^2 q(x)}}$$

SF

Structure function

describes proton structure
probability to find quark with mom. fraction x

Structure Function F_2

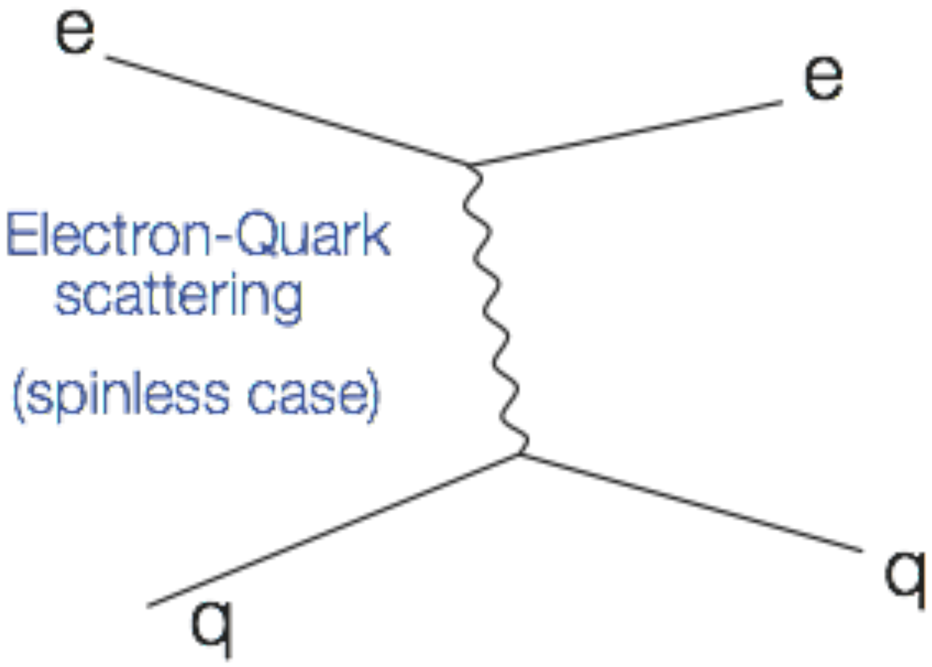

Electron-Quark scattering

(spinless case)

$$\frac{d\sigma(eq)}{dq^2} = \frac{4\pi\alpha^2}{q^4} e_q^2$$

Rutherford scattering on pointlike target

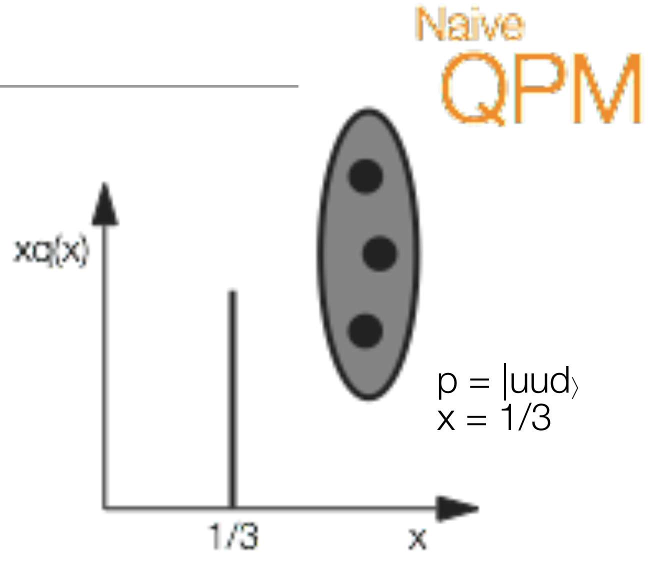

$$\frac{d\sigma(ep)}{dq^2} = \frac{4\pi\alpha^2}{q^4}[2e_u^2 + e_d^2] = \frac{4\pi\alpha^2}{q^4}$$

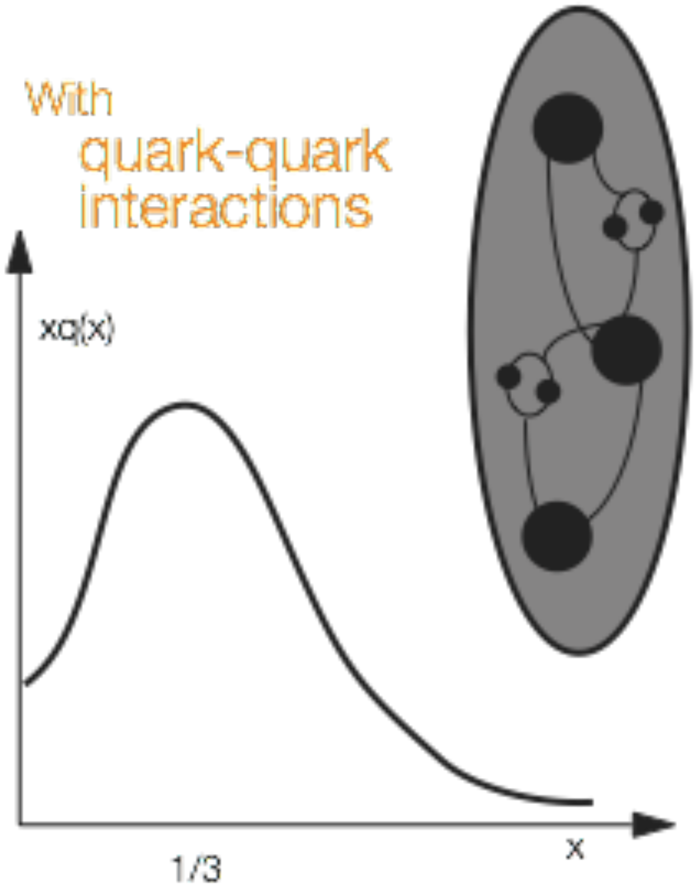

$$\frac{d\sigma(ep)}{dx\,dq^2} = \frac{4\pi\alpha^2}{q^4}[e_u^2 u(x) + e_d^2 d(x) + \ldots]$$

$$= \frac{4\pi\alpha^2}{q^4} \frac{F_2(x)}{x}$$

QPM: Structure Functions F_2 independent of Q^2

Proton

Three
valence quarks

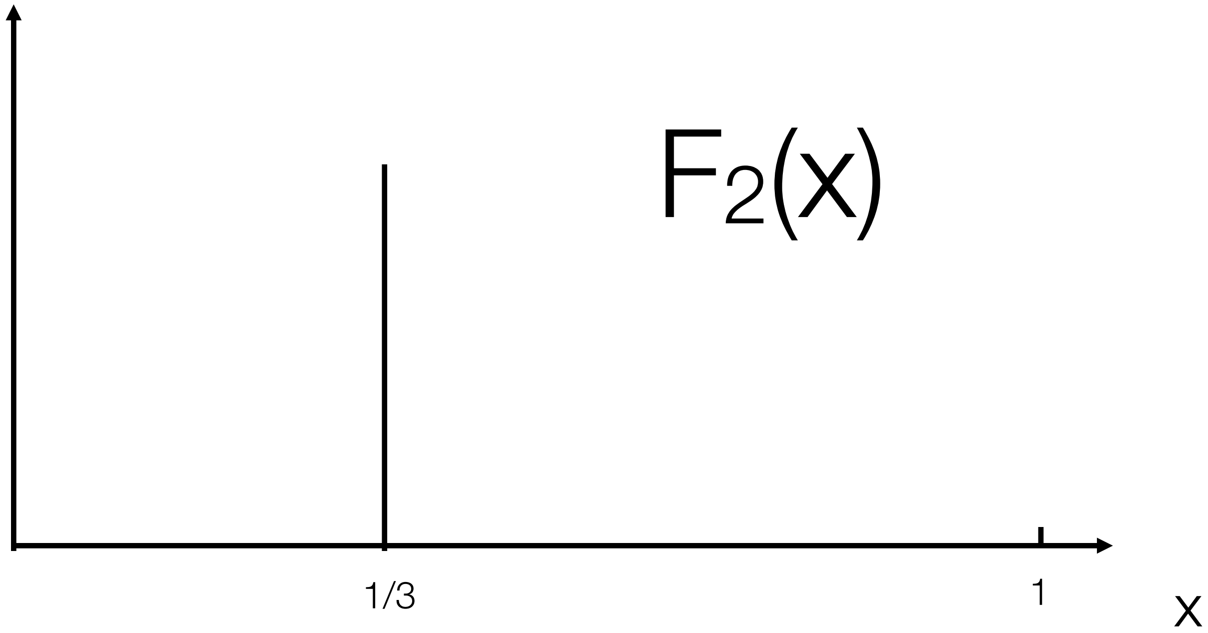

Proton

Three bound
valence quarks

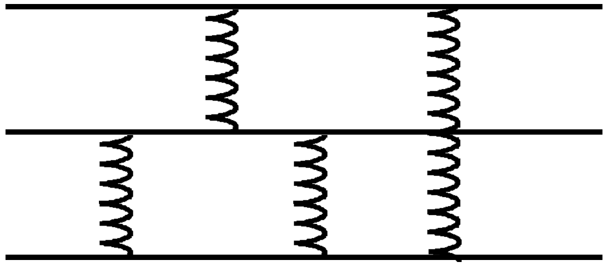

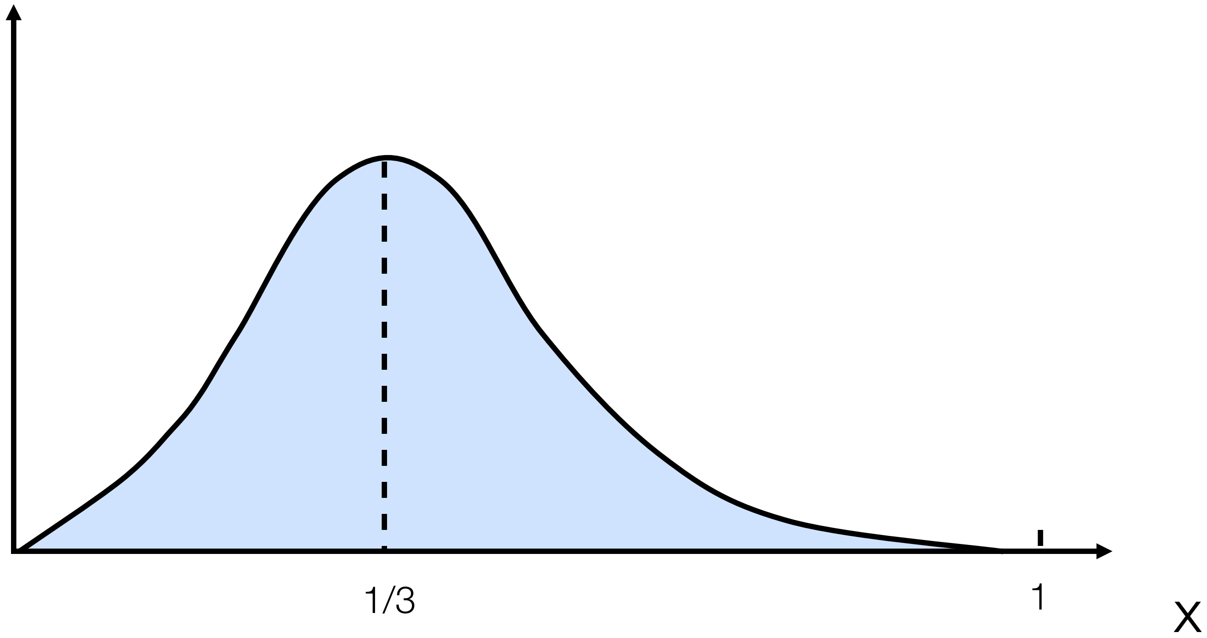

Proton

Bound valence
quarks + gluon radiation

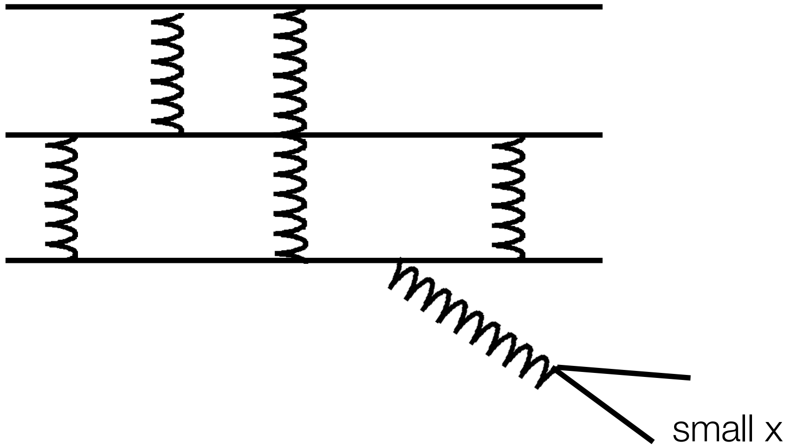

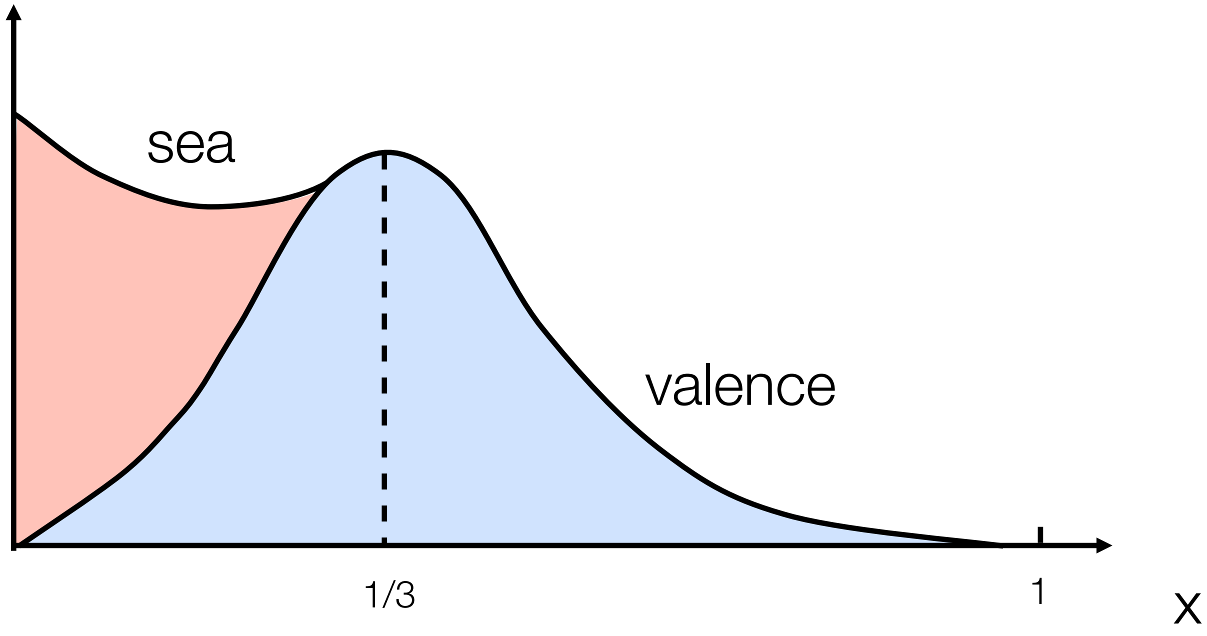

[see e.g. Halzen/Martin]

ep Scattering at HERA

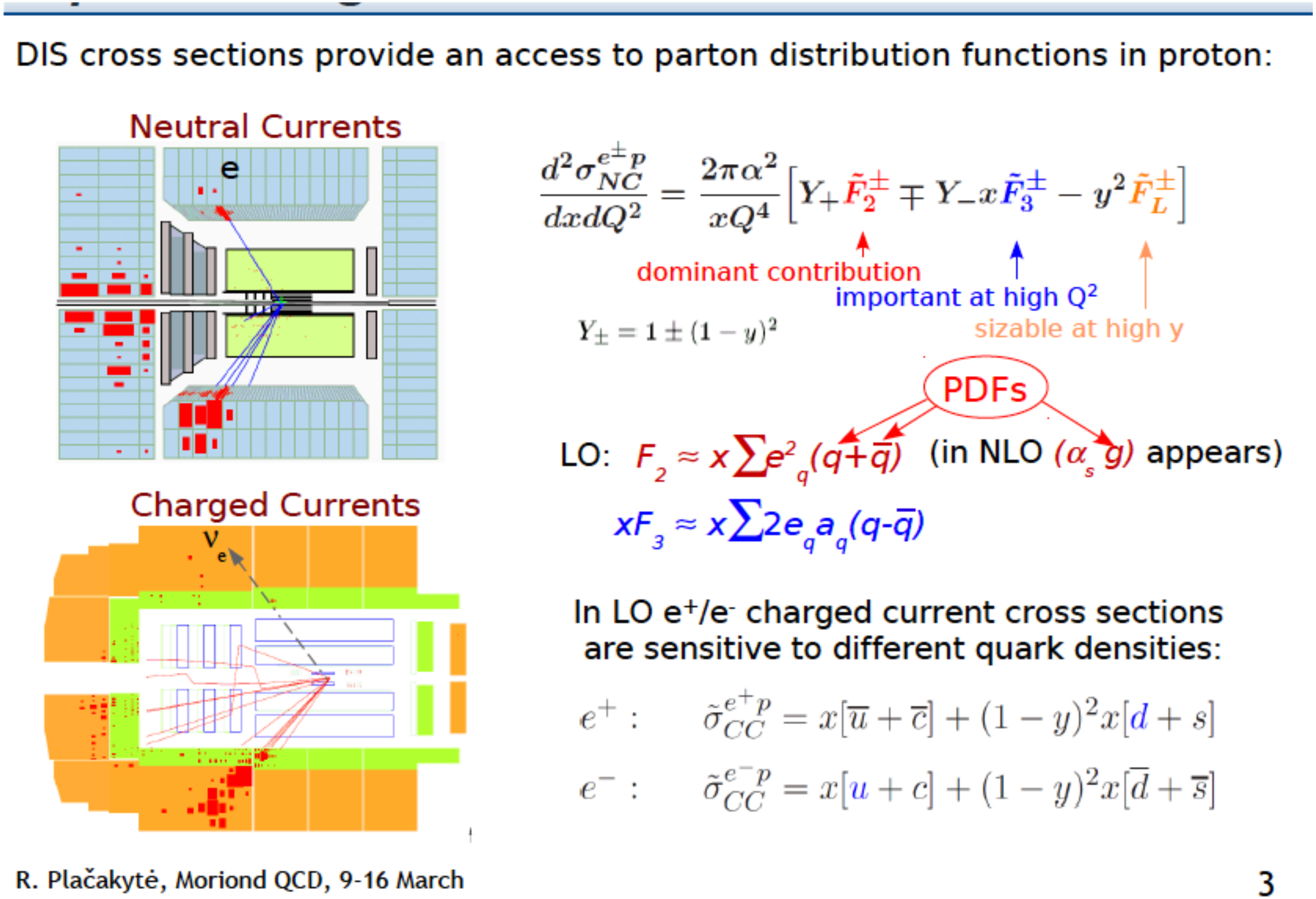

DIS cross sections provide an access to parton distribution functions in proton:

Neutral Currents

Charged Currents

$$\frac{d^2\sigma_{NC}^{e^\pm p}}{dxdQ^2} = \frac{2\pi\alpha^2}{xQ^4}\left[Y_+\tilde{F}_2^\pm \mp Y_- x\tilde{F}_3^\pm - y^2\tilde{F}_L^\pm\right]$$

dominant contribution

important at high Q^2

sizable at high y

$Y_\pm = 1 \pm (1-y)^2$

PDFs

LO: $F_2 \approx x\sum e_q^2(q+\bar{q})$ (in NLO $(\alpha_s g)$ appears)

$xF_3 \approx x\sum 2e_q a_q(q-\bar{q})$

In LO e^+/e^- charged current cross sections are sensitive to different quark densities:

$$e^+ : \quad \tilde{\sigma}_{CC}^{e^+p} = x[\overline{u}+\overline{c}] + (1-y)^2 x[d+s]$$

$$e^- : \quad \tilde{\sigma}_{CC}^{e^-p} = x[u+c] + (1-y)^2 x[\overline{d}+\overline{s}]$$

Which region x-Q^2 is seen by different experiments?

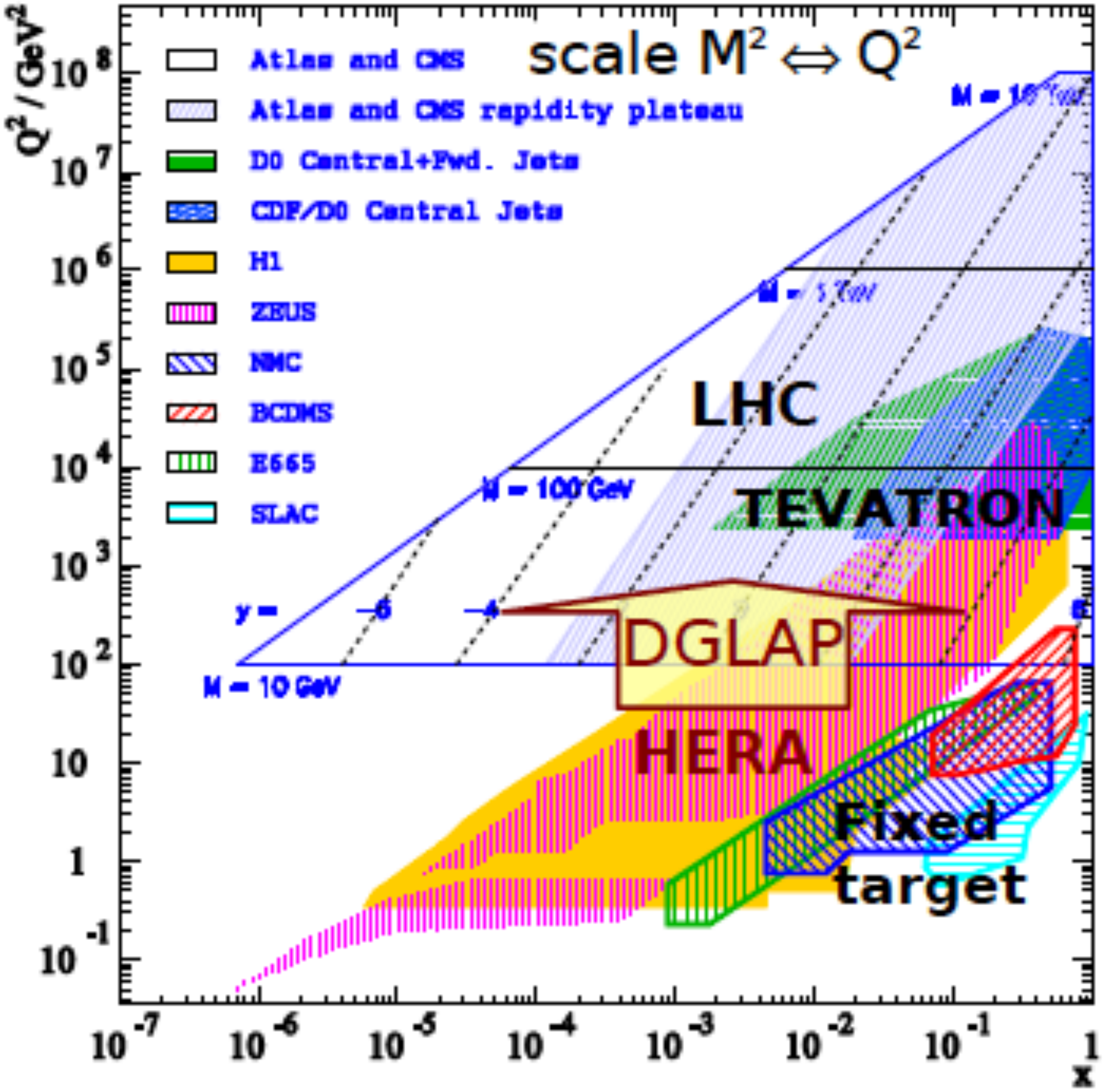

Kinematics of DIS - 1

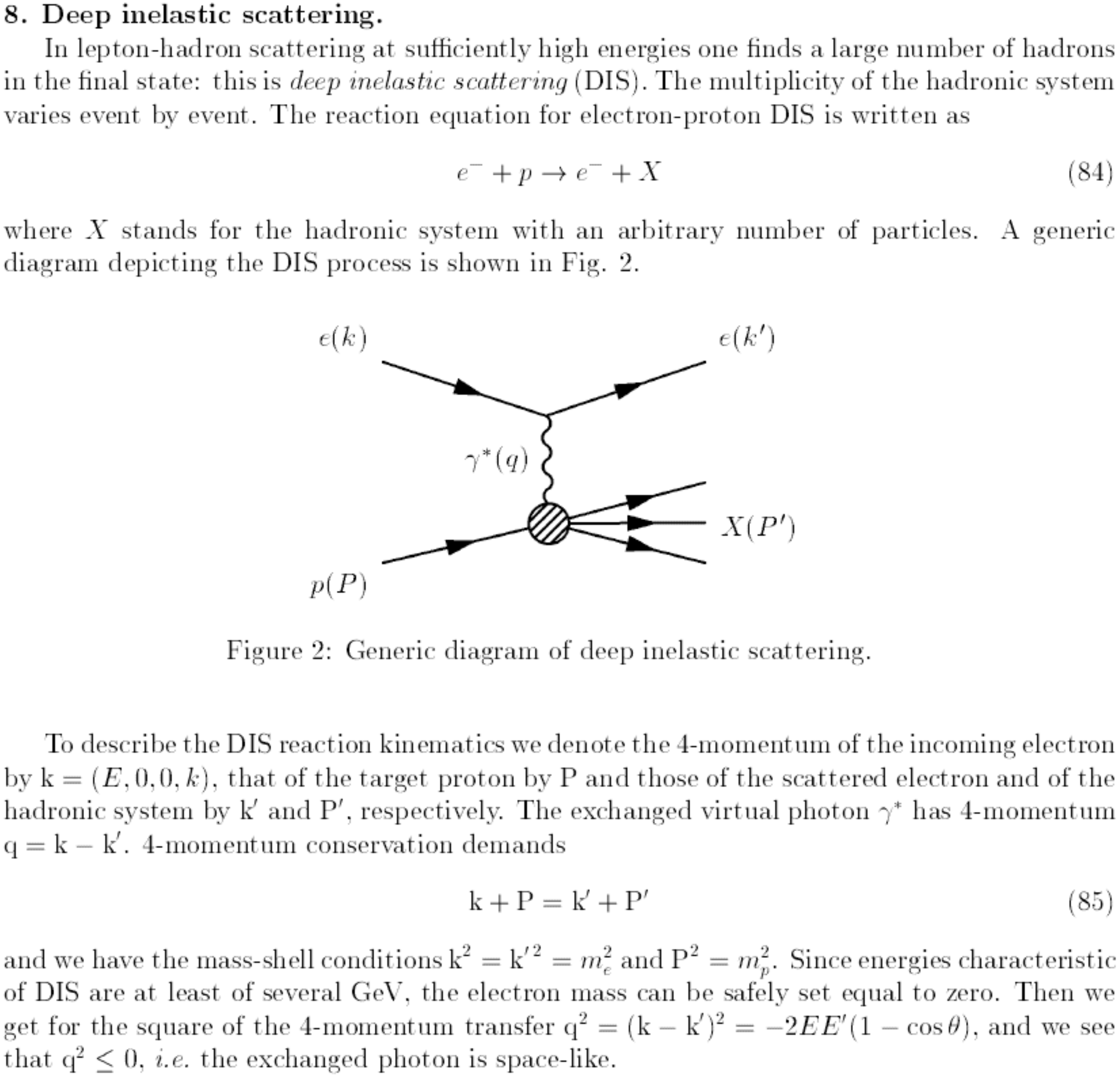

8. Deep inelastic scattering.

In lepton-hadron scattering at sufficiently high energies one finds a large number of hadrons in the final state: this is *deep inelastic scattering* (DIS). The multiplicity of the hadronic system varies event by event. The reaction equation for electron-proton DIS is written as

$$e^- + p \to e^- + X \tag{84}$$

where X stands for the hadronic system with an arbitrary number of particles. A generic diagram depicting the DIS process is shown in Fig. 2.

Figure 2: Generic diagram of deep inelastic scattering.

To describe the DIS reaction kinematics we denote the 4-momentum of the incoming electron by $\mathrm{k} = (E, 0, 0, k)$, that of the target proton by P and those of the scattered electron and of the hadronic system by k' and P', respectively. The exchanged virtual photon γ^* has 4-momentum $\mathrm{q} = \mathrm{k} - \mathrm{k}'$. 4-momentum conservation demands

$$\mathrm{k} + \mathrm{P} = \mathrm{k}' + \mathrm{P}' \tag{85}$$

and we have the mass-shell conditions $\mathrm{k}^2 = \mathrm{k}'^2 = m_e^2$ and $\mathrm{P}^2 = m_p^2$. Since energies characteristic of DIS are at least of several GeV, the electron mass can be safely set equal to zero. Then we get for the square of the 4-momentum transfer $\mathrm{q}^2 = (\mathrm{k} - \mathrm{k}')^2 = -2EE'(1 - \cos\theta)$, and we see that $\mathrm{q}^2 \leq 0$, *i.e.* the exchanged photon is space-like.

Kinematics of DIS - 2

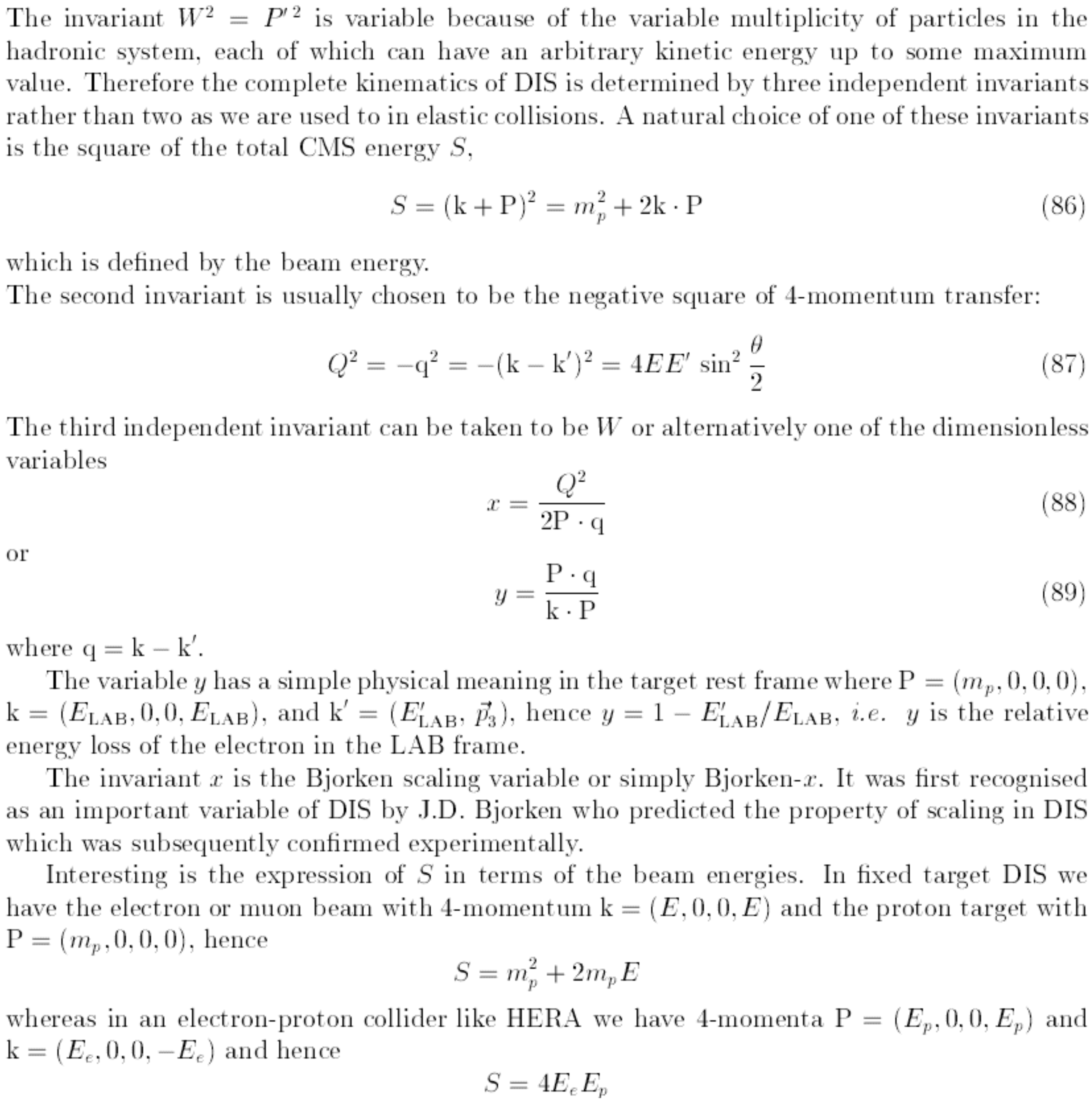

The invariant $W^2 = P'^2$ is variable because of the variable multiplicity of particles in the hadronic system, each of which can have an arbitrary kinetic energy up to some maximum value. Therefore the complete kinematics of DIS is determined by three independent invariants rather than two as we are used to in elastic collisions. A natural choice of one of these invariants is the square of the total CMS energy S,

$$S = (\mathrm{k} + \mathrm{P})^2 = m_p^2 + 2\mathrm{k} \cdot \mathrm{P} \tag{86}$$

which is defined by the beam energy.
The second invariant is usually chosen to be the negative square of 4-momentum transfer:

$$Q^2 = -\mathrm{q}^2 = -(\mathrm{k} - \mathrm{k}')^2 = 4EE' \sin^2 \frac{\theta}{2} \tag{87}$$

The third independent invariant can be taken to be W or alternatively one of the dimensionless variables

$$x = \frac{Q^2}{2\mathrm{P} \cdot \mathrm{q}} \tag{88}$$

or

$$y = \frac{\mathrm{P} \cdot \mathrm{q}}{\mathrm{k} \cdot \mathrm{P}} \tag{89}$$

where $\mathrm{q} = \mathrm{k} - \mathrm{k}'$.

The variable y has a simple physical meaning in the target rest frame where $\mathrm{P} = (m_p, 0, 0, 0)$, $\mathrm{k} = (E_{\mathrm{LAB}}, 0, 0, E_{\mathrm{LAB}})$, and $\mathrm{k}' = (E'_{\mathrm{LAB}}, \vec{p}_3)$, hence $y = 1 - E'_{\mathrm{LAB}}/E_{\mathrm{LAB}}$, *i.e.* y is the relative energy loss of the electron in the LAB frame.

The invariant x is the Bjorken scaling variable or simply Bjorken-x. It was first recognised as an important variable of DIS by J.D. Bjorken who predicted the property of scaling in DIS which was subsequently confirmed experimentally.

Interesting is the expression of S in terms of the beam energies. In fixed target DIS we have the electron or muon beam with 4-momentum $\mathrm{k} = (E, 0, 0, E)$ and the proton target with $\mathrm{P} = (m_p, 0, 0, 0)$, hence

$$S = m_p^2 + 2m_pE$$

whereas in an electron-proton collider like HERA we have 4-momenta $\mathrm{P} = (E_p, 0, 0, E_p)$ and $\mathrm{k} = (E_e, 0, 0, -E_e)$ and hence

$$S = 4E_eE_p$$

Kinematics of DIS - 3

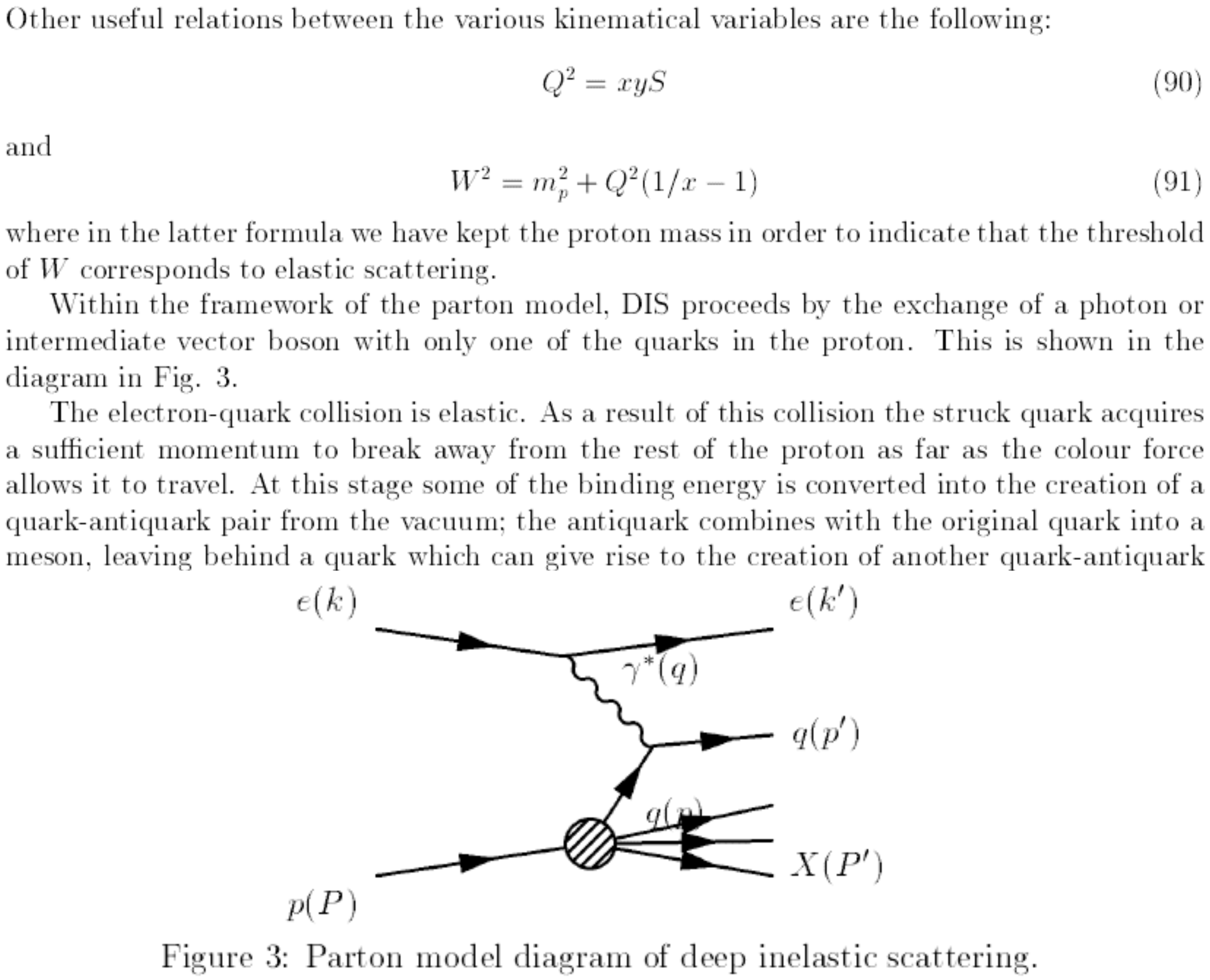

Other useful relations between the various kinematical variables are the following:

$$Q^2 = xyS \tag{90}$$

and

$$W^2 = m_p^2 + Q^2(1/x - 1) \tag{91}$$

where in the latter formula we have kept the proton mass in order to indicate that the threshold of W corresponds to elastic scattering.

Within the framework of the parton model, DIS proceeds by the exchange of a photon or intermediate vector boson with only one of the quarks in the proton. This is shown in the diagram in Fig. 3.

The electron-quark collision is elastic. As a result of this collision the struck quark acquires a sufficient momentum to break away from the rest of the proton as far as the colour force allows it to travel. At this stage some of the binding energy is converted into the creation of a quark-antiquark pair from the vacuum; the antiquark combines with the original quark into a meson, leaving behind a quark which can give rise to the creation of another quark-antiquark

Figure 3: Parton model diagram of deep inelastic scattering.

Kinematics of DIS - 4

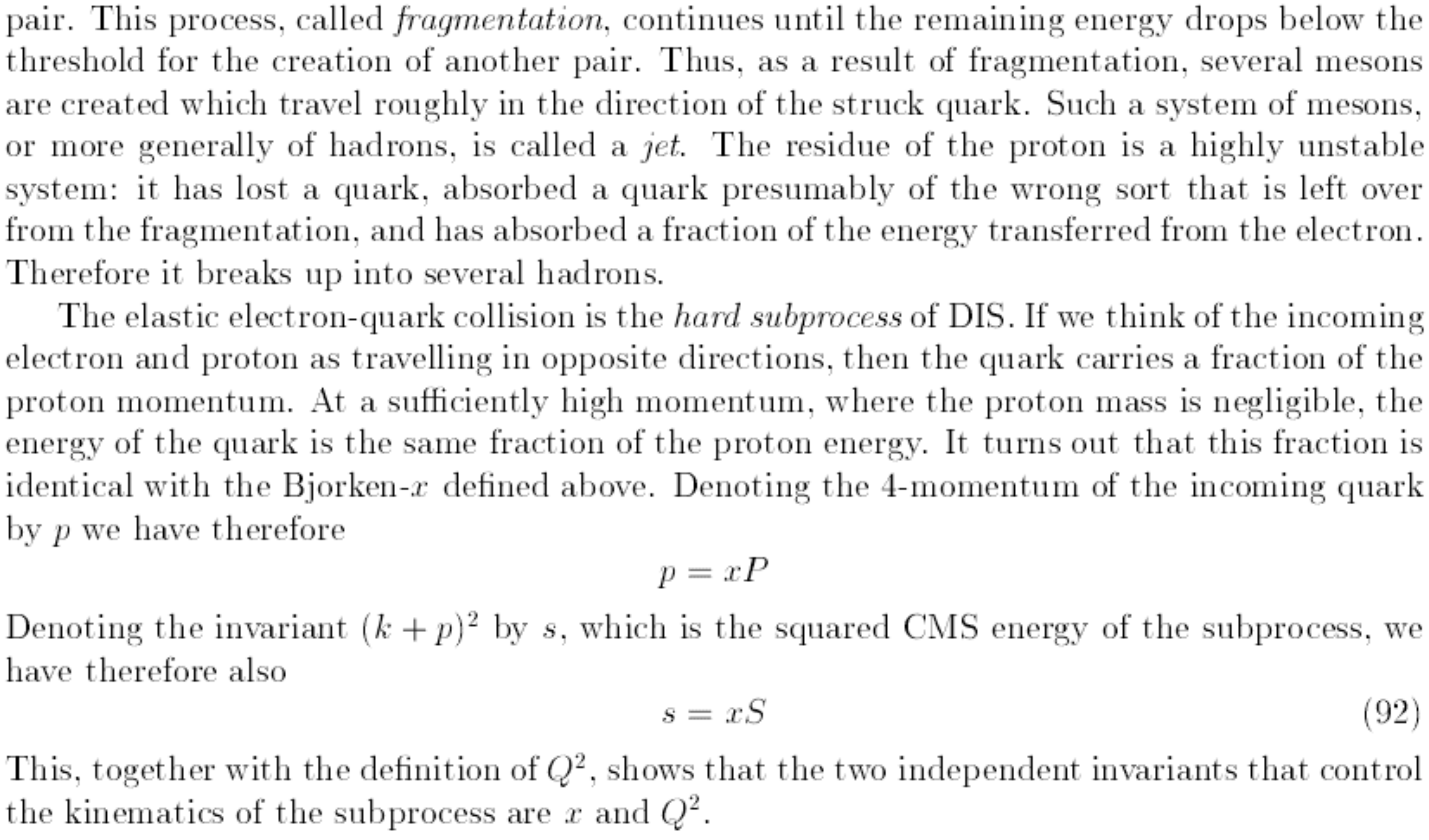

pair. This process, called *fragmentation*, continues until the remaining energy drops below the threshold for the creation of another pair. Thus, as a result of fragmentation, several mesons are created which travel roughly in the direction of the struck quark. Such a system of mesons, or more generally of hadrons, is called a *jet*. The residue of the proton is a highly unstable system: it has lost a quark, absorbed a quark presumably of the wrong sort that is left over from the fragmentation, and has absorbed a fraction of the energy transferred from the electron. Therefore it breaks up into several hadrons.

The elastic electron-quark collision is the *hard subprocess* of DIS. If we think of the incoming electron and proton as travelling in opposite directions, then the quark carries a fraction of the proton momentum. At a sufficiently high momentum, where the proton mass is negligible, the energy of the quark is the same fraction of the proton energy. It turns out that this fraction is identical with the Bjorken-x defined above. Denoting the 4-momentum of the incoming quark by p we have therefore

$$p = xP$$

Denoting the invariant $(k + p)^2$ by s, which is the squared CMS energy of the subprocess, we have therefore also

$$s = xS \tag{92}$$

This, together with the definition of Q^2, shows that the two independent invariants that control the kinematics of the subprocess are x and Q^2.

Kinematics of DIS - 5

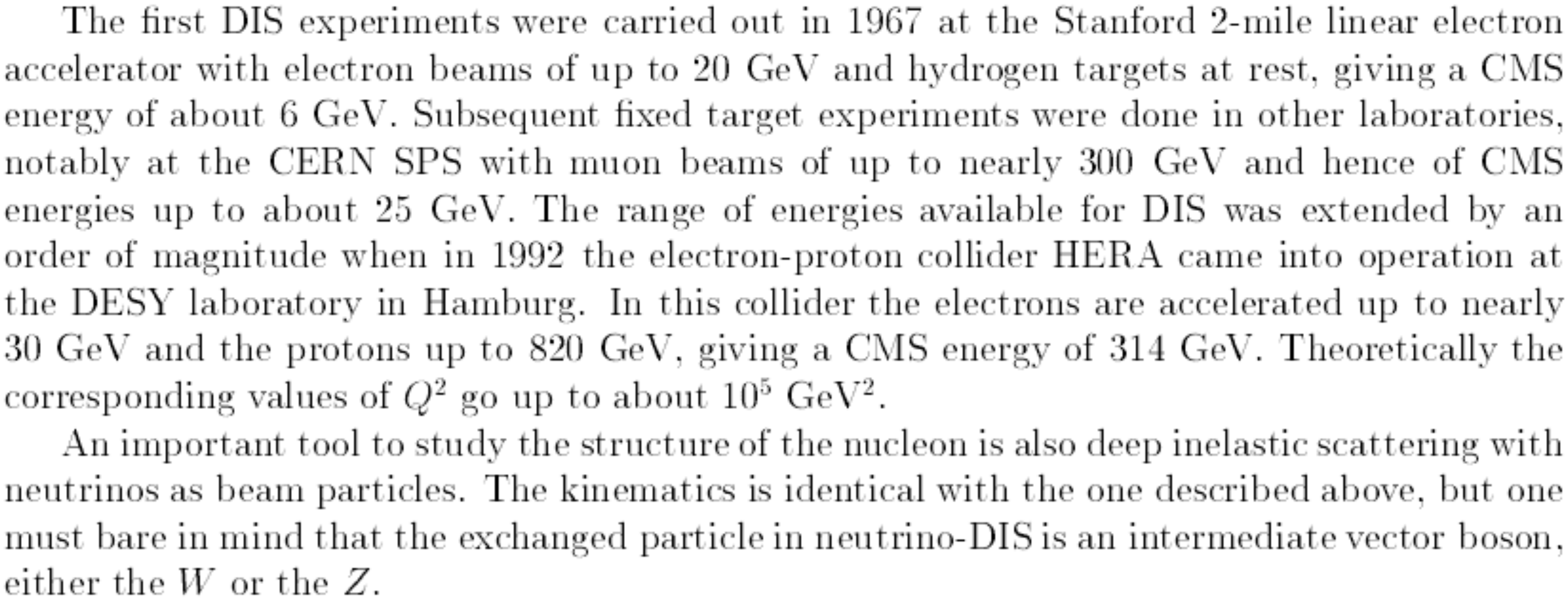

The first DIS experiments were carried out in 1967 at the Stanford 2-mile linear electron accelerator with electron beams of up to 20 GeV and hydrogen targets at rest, giving a CMS energy of about 6 GeV. Subsequent fixed target experiments were done in other laboratories, notably at the CERN SPS with muon beams of up to nearly 300 GeV and hence of CMS energies up to about 25 GeV. The range of energies available for DIS was extended by an order of magnitude when in 1992 the electron-proton collider HERA came into operation at the DESY laboratory in Hamburg. In this collider the electrons are accelerated up to nearly 30 GeV and the protons up to 820 GeV, giving a CMS energy of 314 GeV. Theoretically the corresponding values of Q^2 go up to about 10^5 GeV^2.

An important tool to study the structure of the nucleon is also deep inelastic scattering with neutrinos as beam particles. The kinematics is identical with the one described above, but one must bare in mind that the exchanged particle in neutrino-DIS is an intermediate vector boson, either the W or the Z.

F_1 and F_2

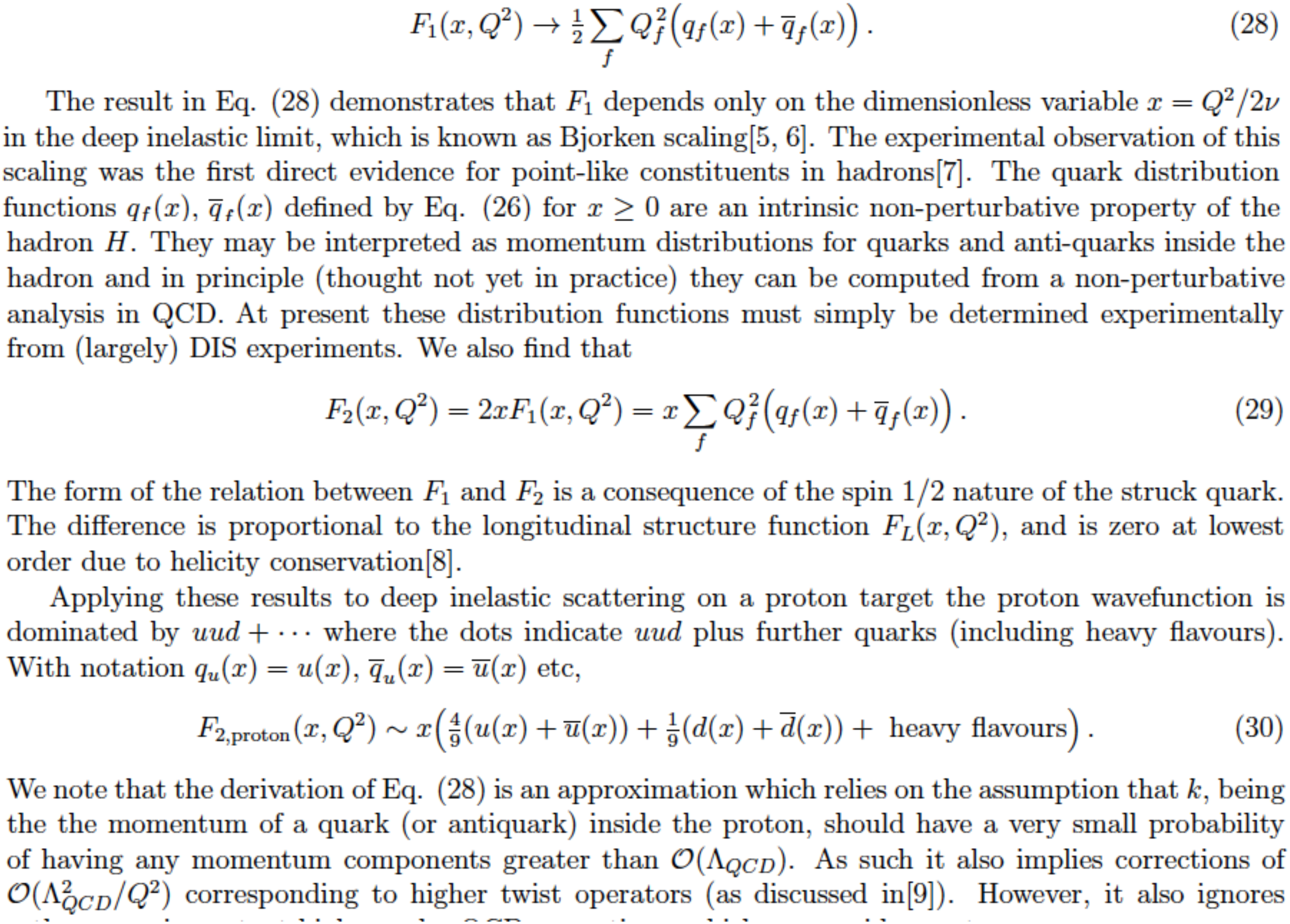

$$F_1(x, Q^2) \to \tfrac{1}{2} \sum_f Q_f^2 \Big(q_f(x) + \overline{q}_f(x) \Big) \, . \tag{28}$$

The result in Eq. (28) demonstrates that F_1 depends only on the dimensionless variable $x = Q^2/2\nu$ in the deep inelastic limit, which is known as Bjorken scaling[5, 6]. The experimental observation of this scaling was the first direct evidence for point-like constituents in hadrons[7]. The quark distribution functions $q_f(x)$, $\overline{q}_f(x)$ defined by Eq. (26) for $x \geq 0$ are an intrinsic non-perturbative property of the hadron H. They may be interpreted as momentum distributions for quarks and anti-quarks inside the hadron and in principle (thought not yet in practice) they can be computed from a non-perturbative analysis in QCD. At present these distribution functions must simply be determined experimentally from (largely) DIS experiments. We also find that

$$F_2(x, Q^2) = 2xF_1(x, Q^2) = x \sum_f Q_f^2 \Big(q_f(x) + \overline{q}_f(x) \Big) \, . \tag{29}$$

The form of the relation between F_1 and F_2 is a consequence of the spin 1/2 nature of the struck quark. The difference is proportional to the longitudinal structure function $F_L(x, Q^2)$, and is zero at lowest order due to helicity conservation[8].

Applying these results to deep inelastic scattering on a proton target the proton wavefunction is dominated by $uud + \cdots$ where the dots indicate uud plus further quarks (including heavy flavours). With notation $q_u(x) = u(x)$, $\overline{q}_u(x) = \overline{u}(x)$ etc,

$$F_{2,\mathrm{proton}}(x, Q^2) \sim x \Big(\tfrac{4}{9}(u(x) + \overline{u}(x)) + \tfrac{1}{9}(d(x) + \overline{d}(x)) + \text{ heavy flavours} \Big) \, . \tag{30}$$

We note that the derivation of Eq. (28) is an approximation which relies on the assumption that k, being the the momentum of a quark (or antiquark) inside the proton, should have a very small probability of having any momentum components greater than $\mathcal{O}(\Lambda_{QCD})$. As such it also implies corrections of $\mathcal{O}(\Lambda_{QCD}^2/Q^2)$ corresponding to higher twist operators (as discussed in[9]). However, it also ignores

Scaling Behavior [SLAC 1972]

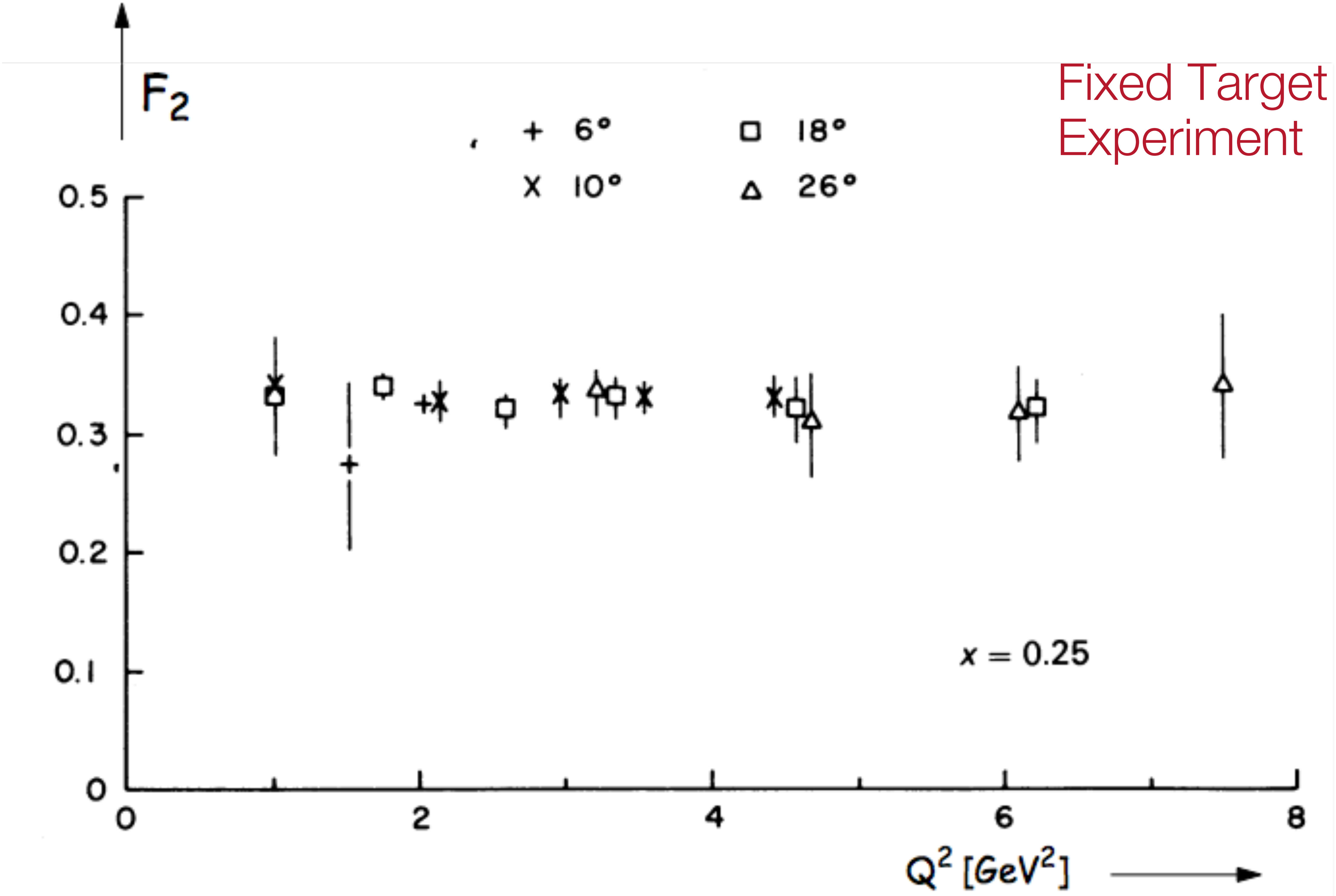

Fixed Target Experiment

Scaling Violations [SLAC 1972]

$$F_2(x,Q^2) = \sum e_q^2 x q(x,Q^2)$$

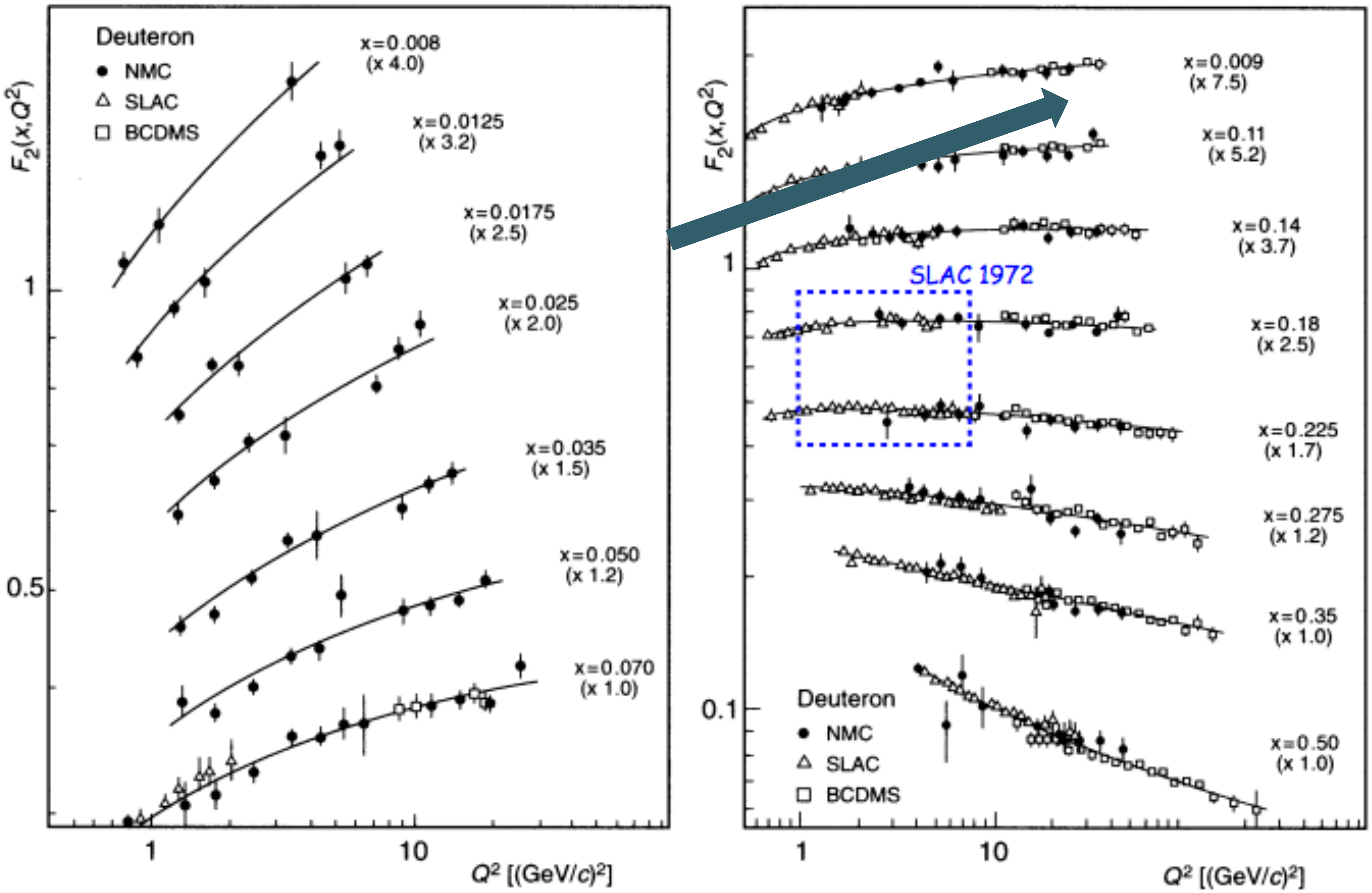

DGLAP Equations

[DGLAP: Dokshitzer, Gribov, Lipatov, Altarelli, Parisi]

$$\frac{4}{3}\left[\frac{1+z^2}{1-z}\right]$$

$$\frac{1}{2}\left[z^2+(1-z^2)\right]$$

PDFs

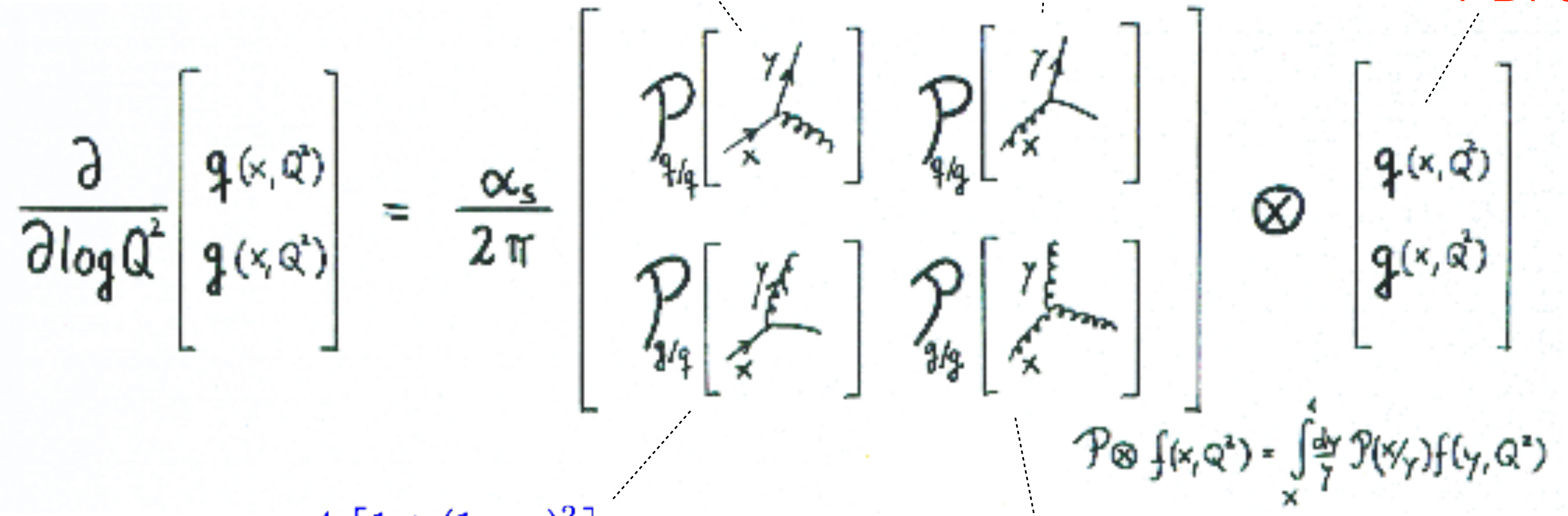

$$\frac{\partial}{\partial \log Q^2}\begin{bmatrix} q(x,Q^2) \\ g(x,Q^2) \end{bmatrix} = \frac{\alpha_s}{2\pi}\begin{bmatrix} \mathcal{P}_{q/q} & \mathcal{P}_{q/g} \\ \mathcal{P}_{g/q} & \mathcal{P}_{g/g} \end{bmatrix} \otimes \begin{bmatrix} q(x,Q^2) \\ g(x,Q^2) \end{bmatrix}$$

$$\mathcal{P}\otimes f(x,Q^2) = \int_x^1 \frac{dy}{y}\,\mathcal{P}(x/y)\,f(y,Q^2)$$

$$\frac{4}{3}\left[\frac{1+(1-z)^2}{z}\right]$$

$$6\left[\frac{z}{1-z}+\frac{1-z}{z}+z(1-z)\right]$$

[z: momentum fraction of radiated parton]

Scaling Violations

[HERA & fixed target data]

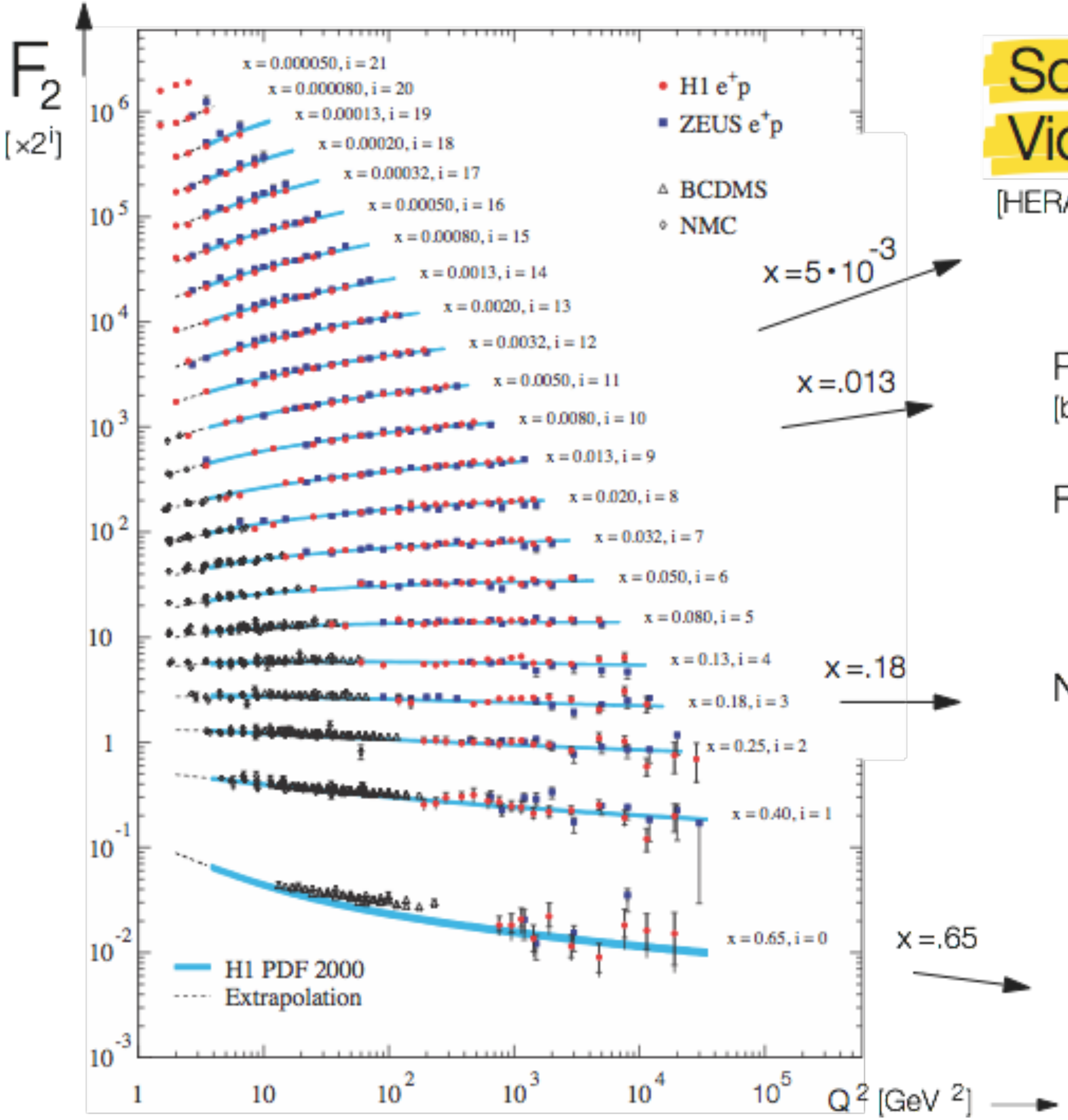

Precision: 2-3%
[bulk region]

For $x < 10^{-2}$:

$$\frac{dF_2}{d\log Q^2} \sim g(x,Q^2) \cdot \alpha_s(Q^2)$$

NLO QCD Fits:

Quark densities
Gluon density
Strong coupling α_s

HERA I

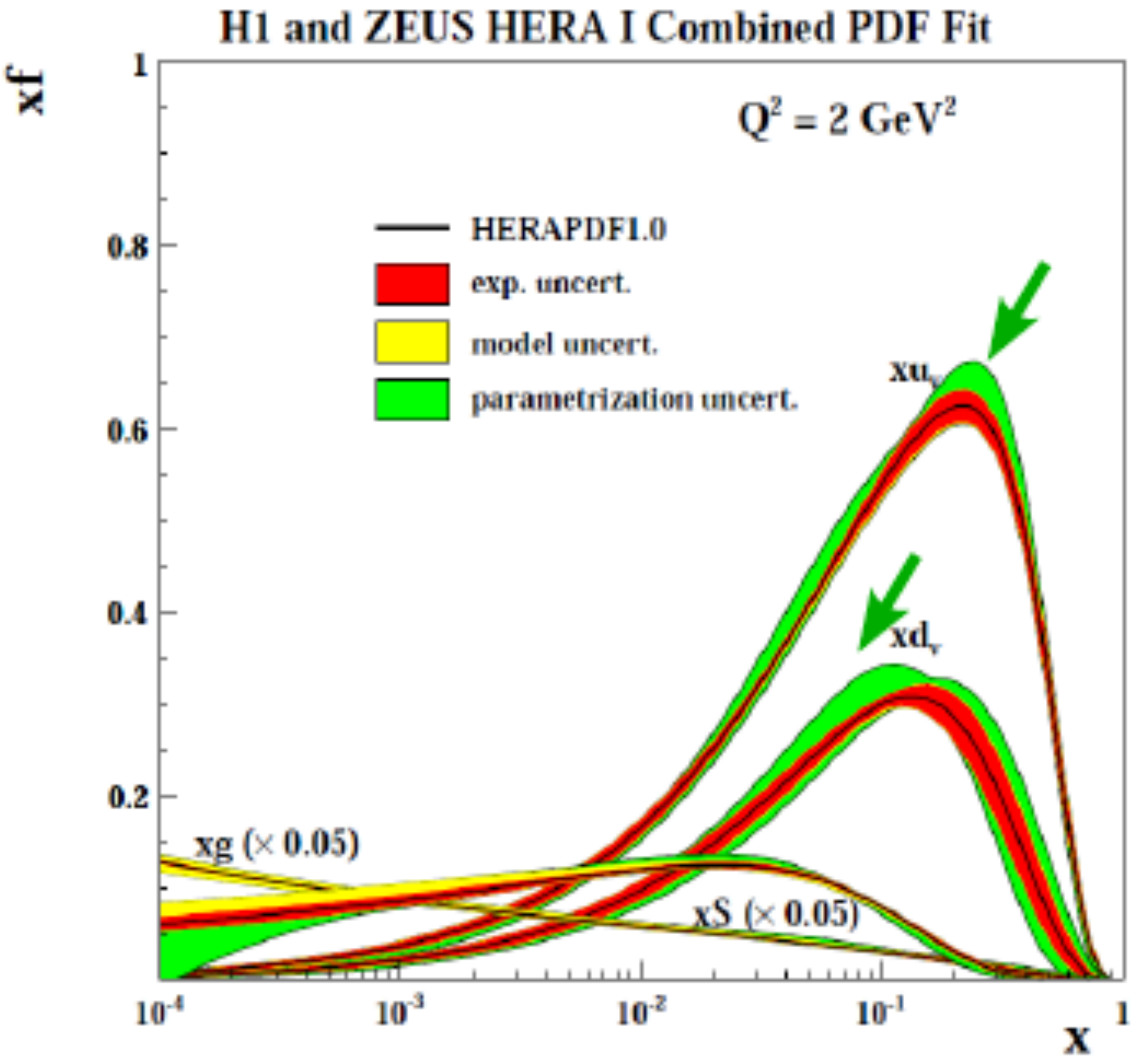

HERA I + II

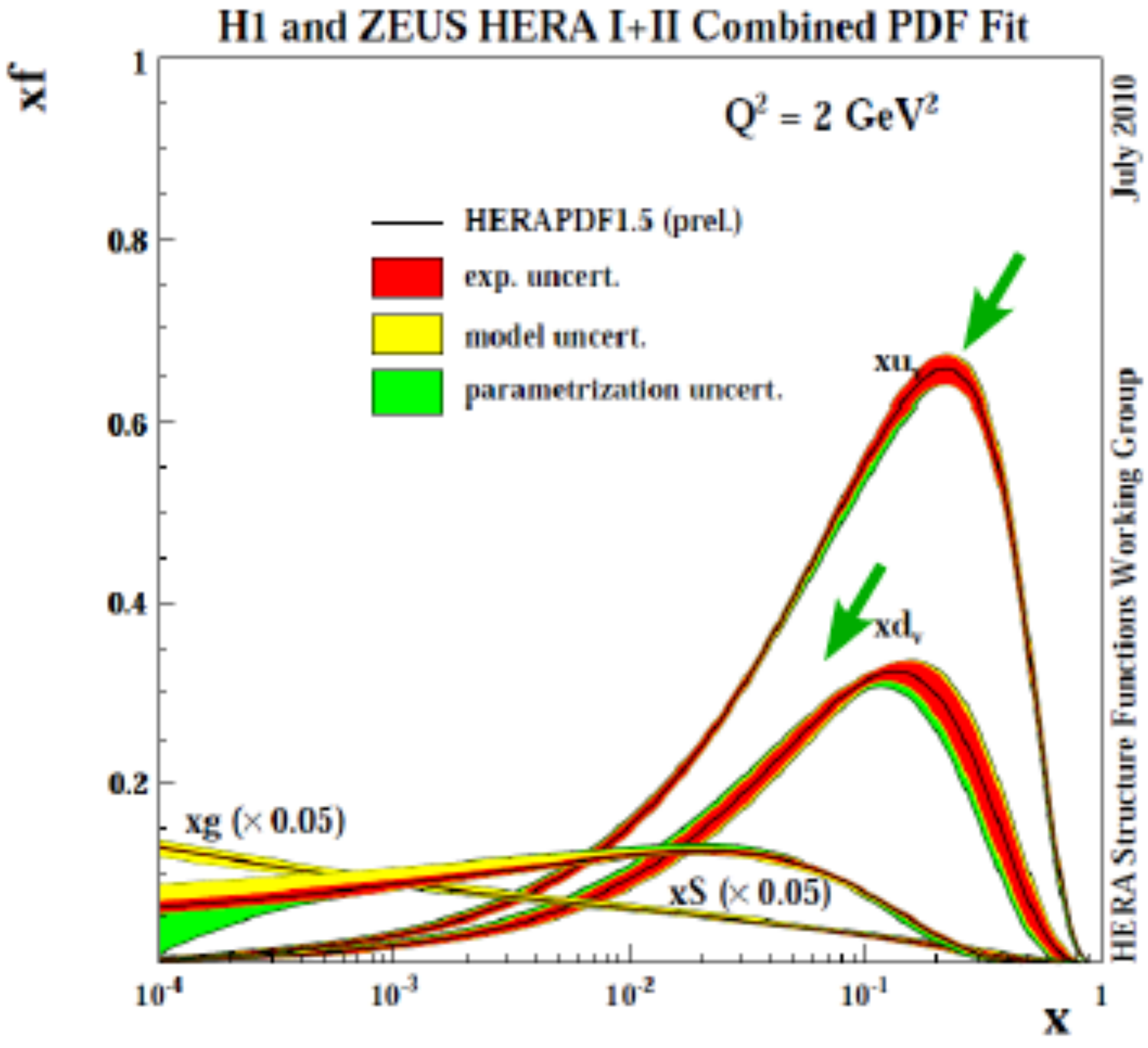

Proton Parton Densities

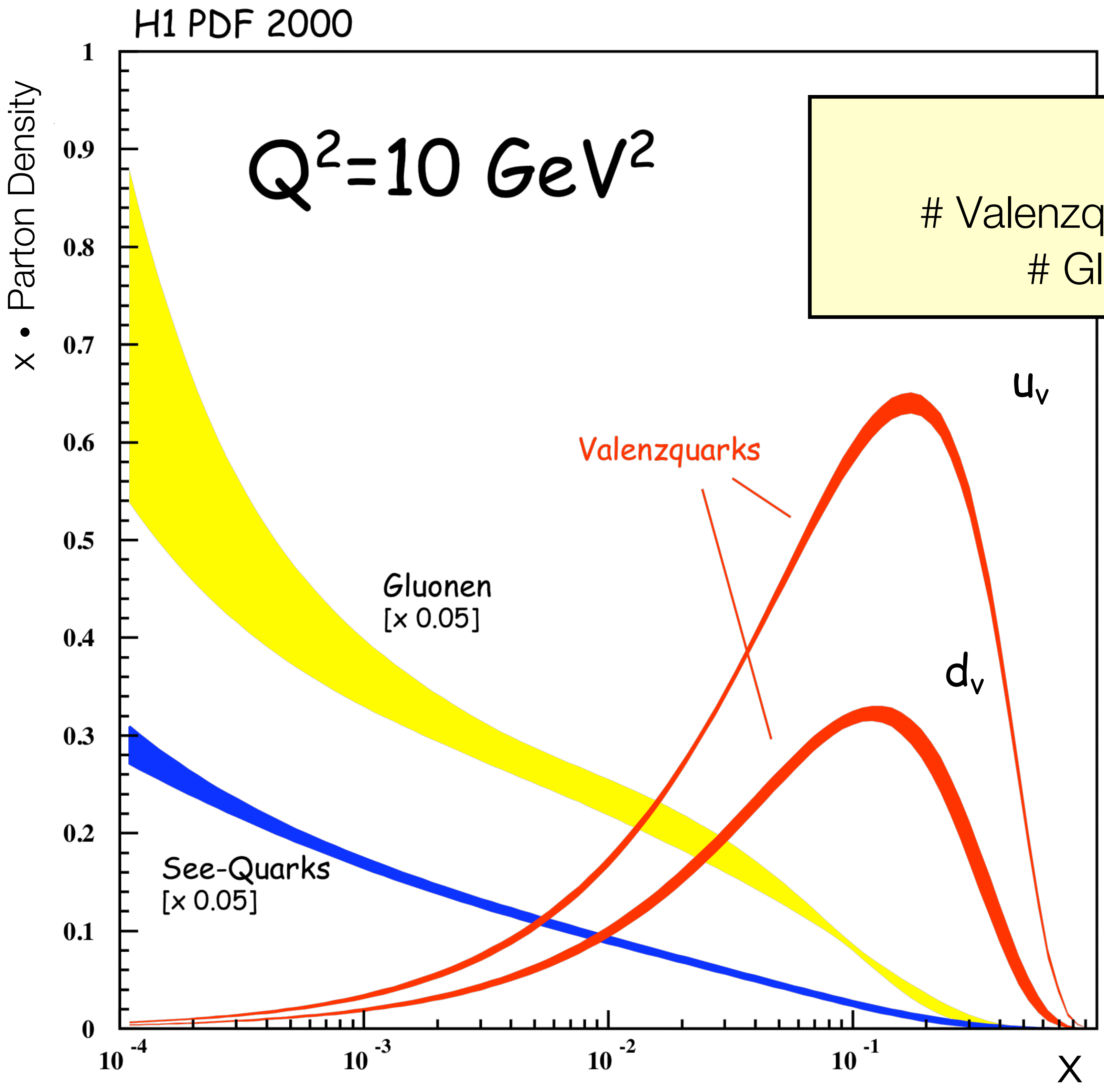

\# Valenzquarks = $\int u_v(x) + d_v(x)\,dx = 3$

\# Gluonen = $\int g(x)\,dx > 30$

Proton
gluon dominated

Proton Parton Densities

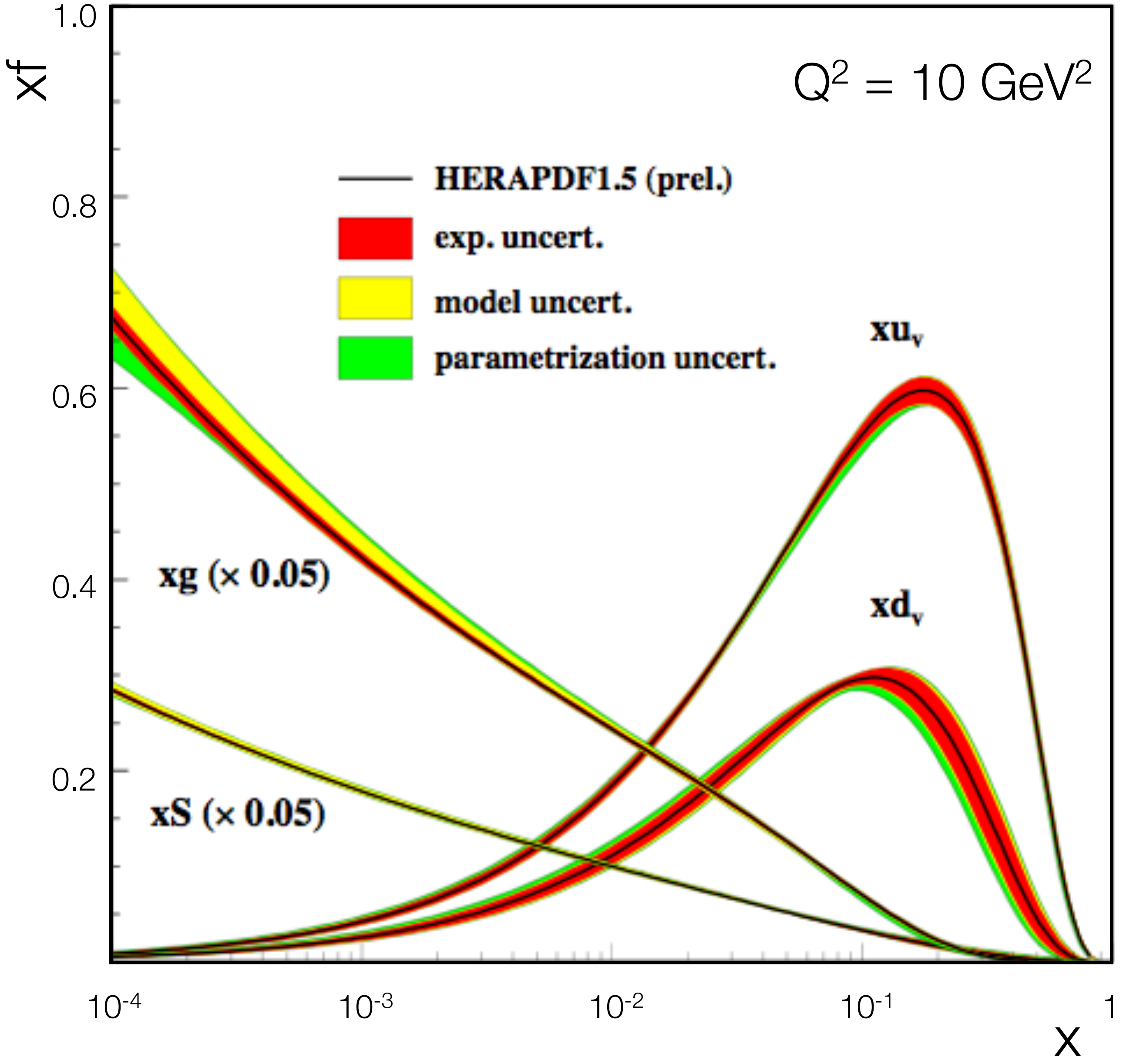
H1 and ZEUS HERA I+II Combined PDF Fit

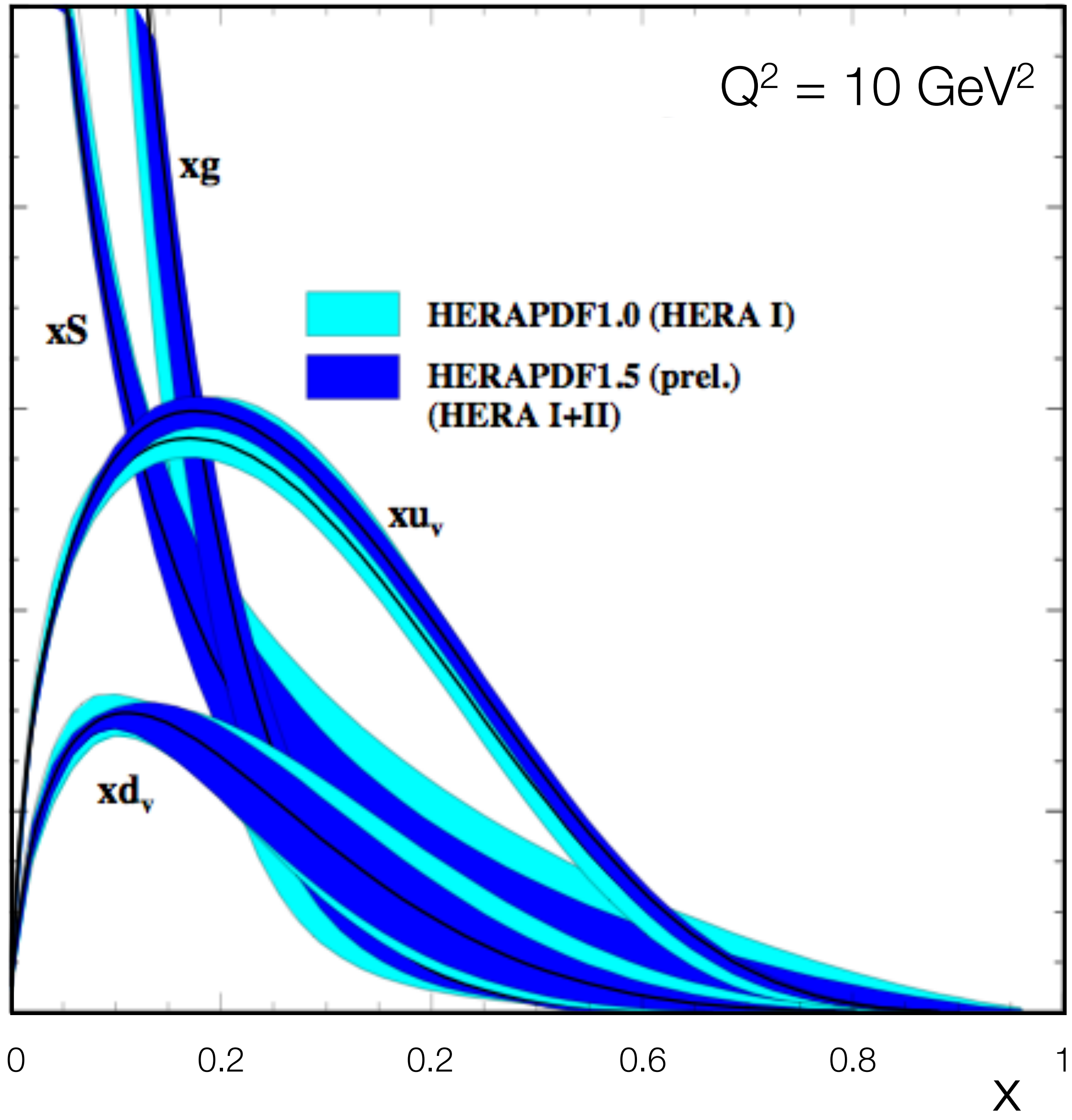
H1 and ZEUS Combined PDF Fit

HERA Structure Functions Working Group July 2010

Proton Parton Densities

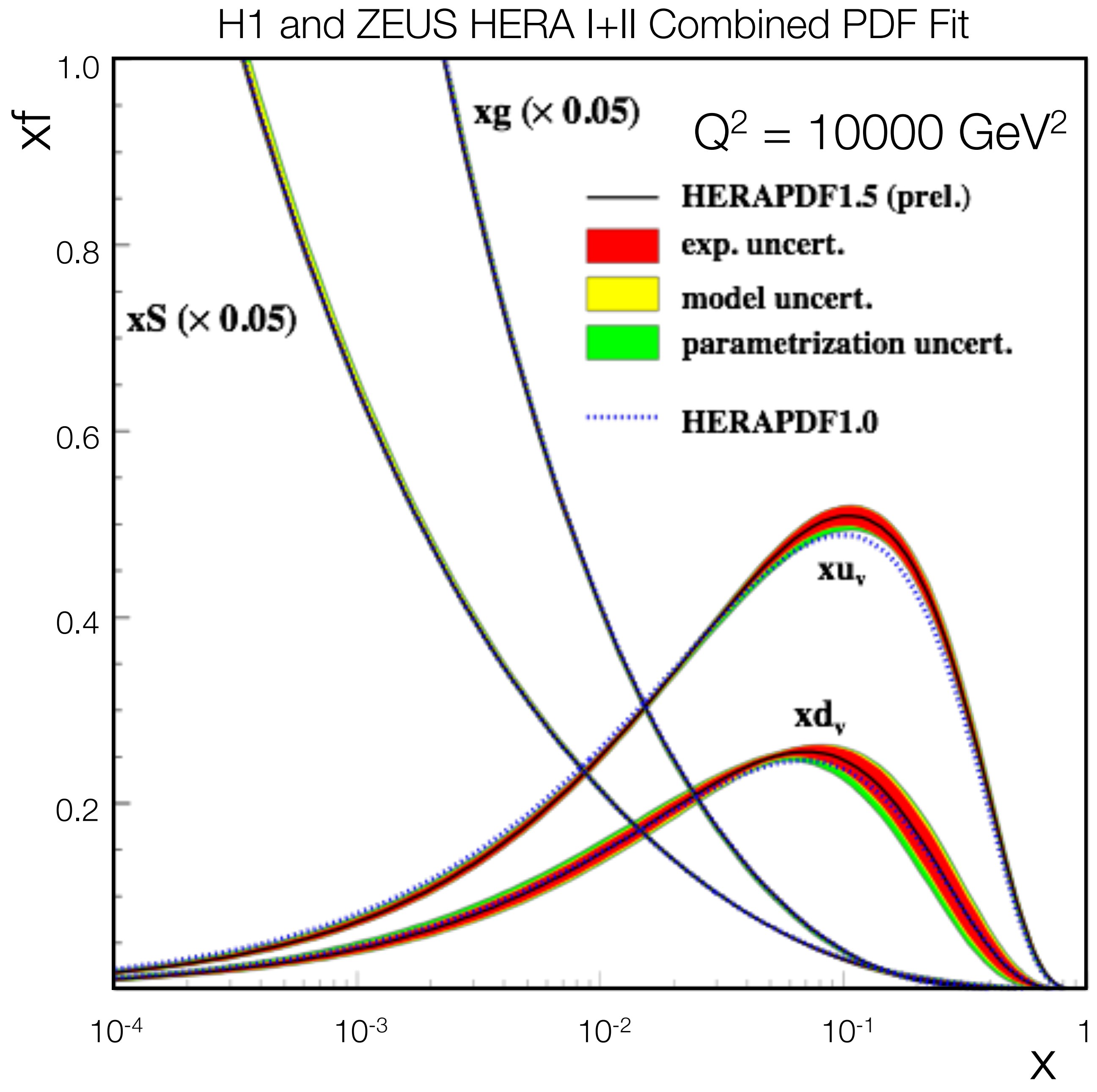

H1 and ZEUS HERA I+II Combined PDF Fit

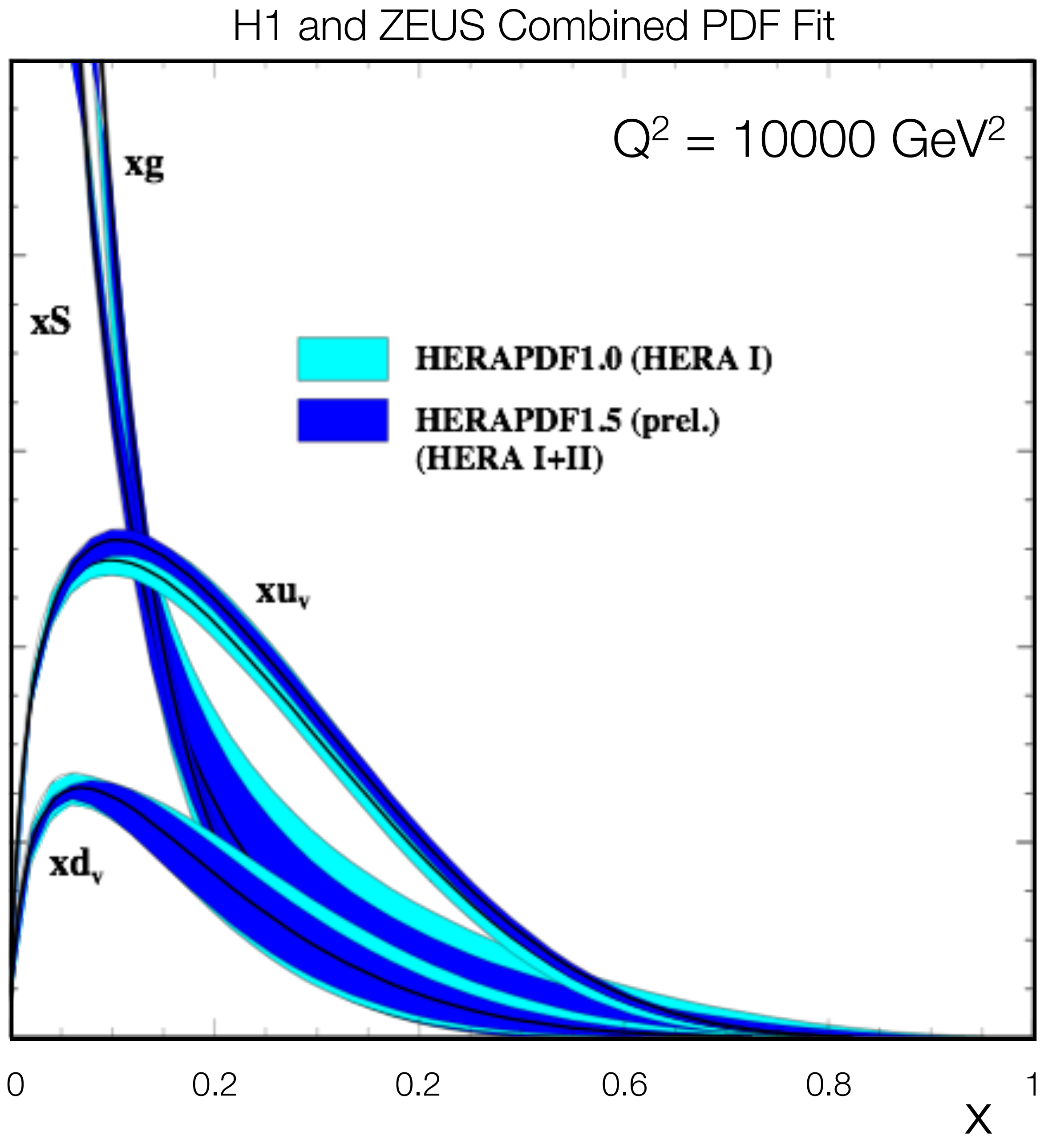

H1 and ZEUS Combined PDF Fit

HERA Structure Functions Working Group July 2010

Parton Distributions @ Q^2 = 10 TeV GeV

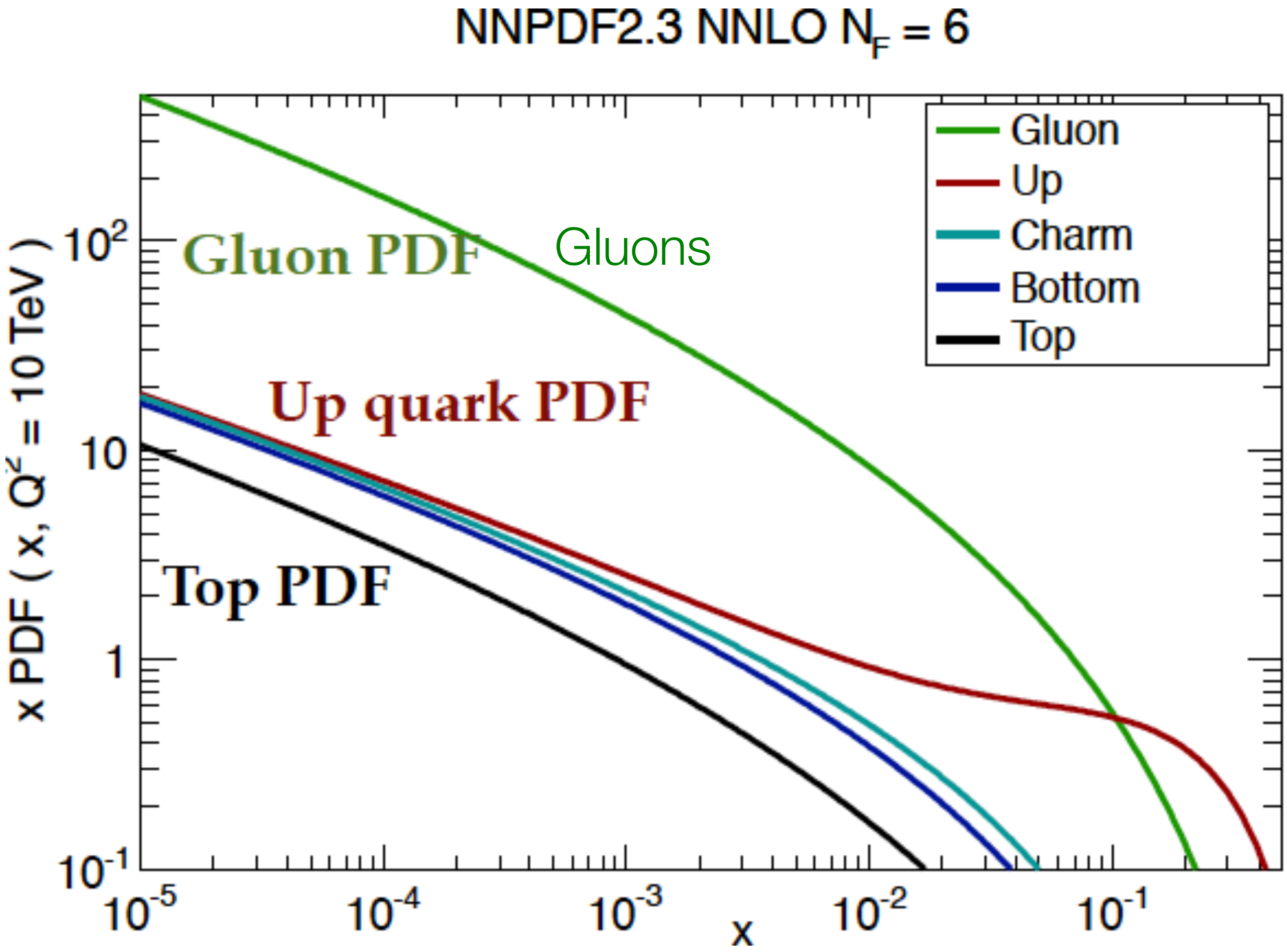

Todays Picture of the Proton

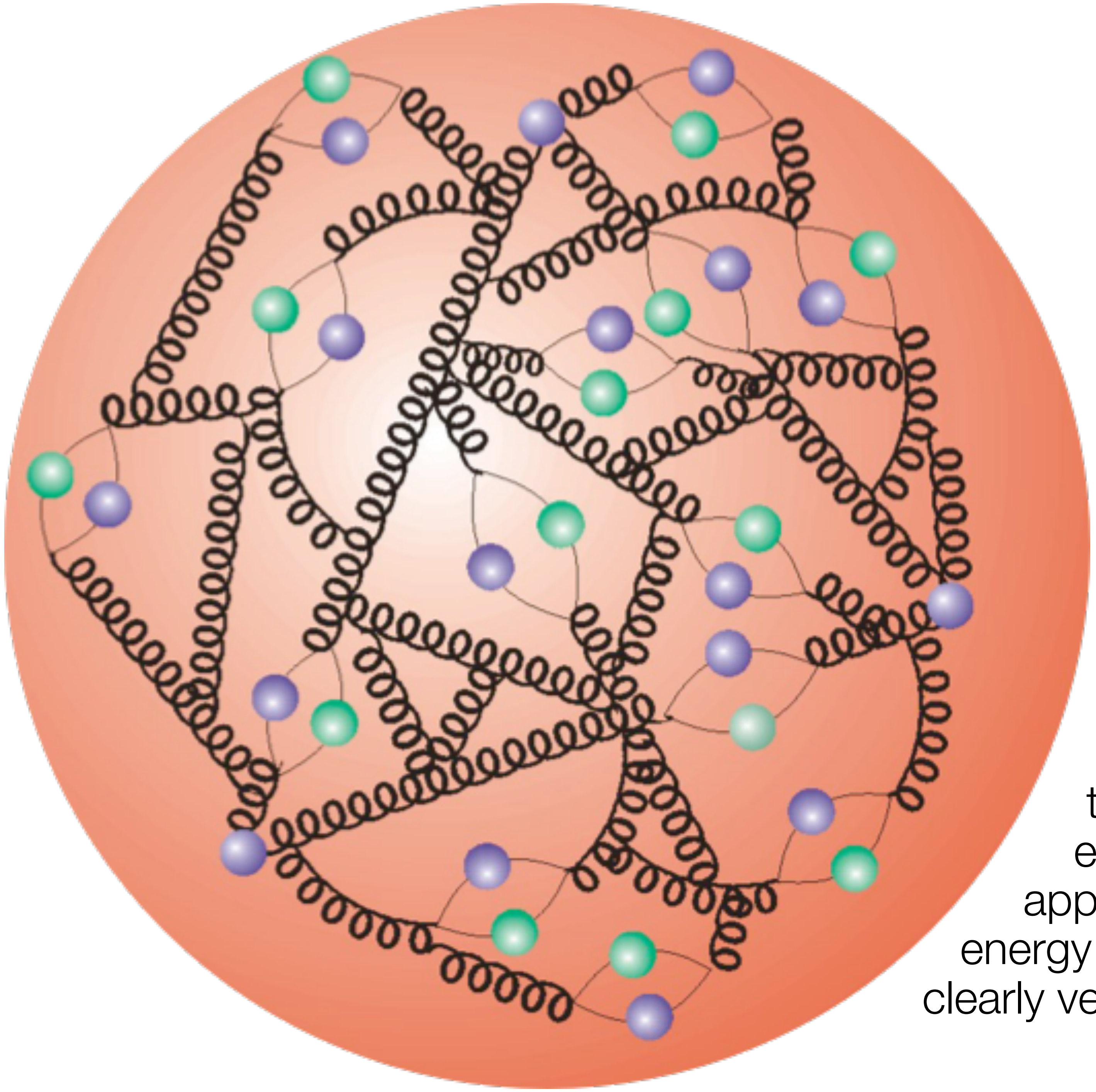

The most dramatic of these [experimental consequences], that the protons viewed at ever higher resolution would appear more and more as field energy (soft glue), was only clearly verified at HERA ...

F. Wilczek
[Nobel Prize 2004]

Proton-Proton Scattering @ LHC

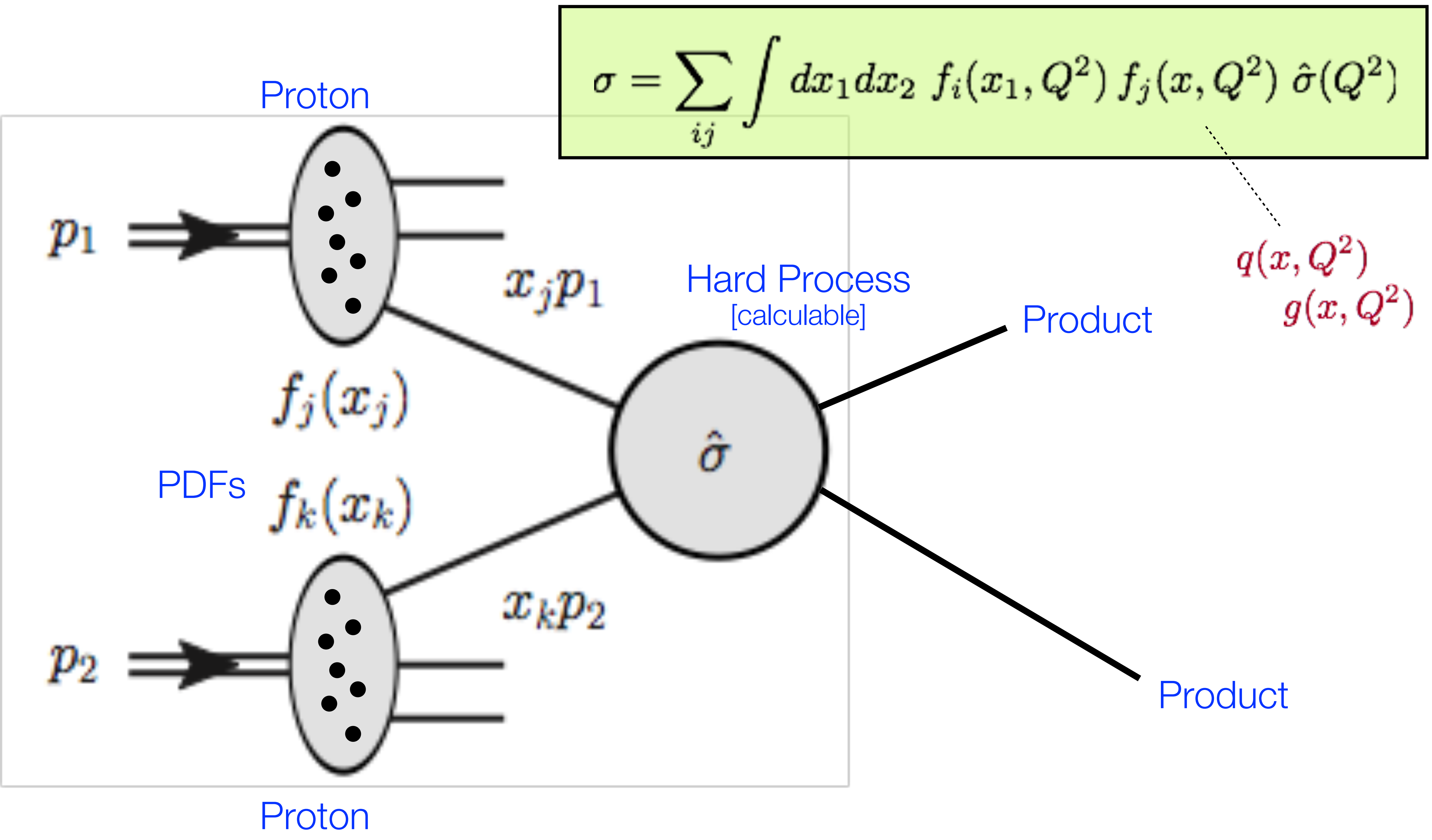

$$\sigma = \sum_{ij} \int dx_1 dx_2 \ f_i(x_1, Q^2) \, f_j(x, Q^2) \, \hat{\sigma}(Q^2)$$

$q(x, Q^2)$

$g(x, Q^2)$

Proton

p_1

$x_j p_1$

Hard Process

[calculable]

Product

$f_j(x_j)$

$\hat{\sigma}$

PDFs

$f_k(x_k)$

$x_k p_2$

p_2

Product

Proton

Proton-Proton Scattering @ LHC

$$\sigma = \sum_{ij} \int dx_1 dx_2 \; f_i(x_1, Q^2) \, f_j(x, Q^2) \; \hat{\sigma}(Q^2)$$

$\otimes$ **Hadronization**

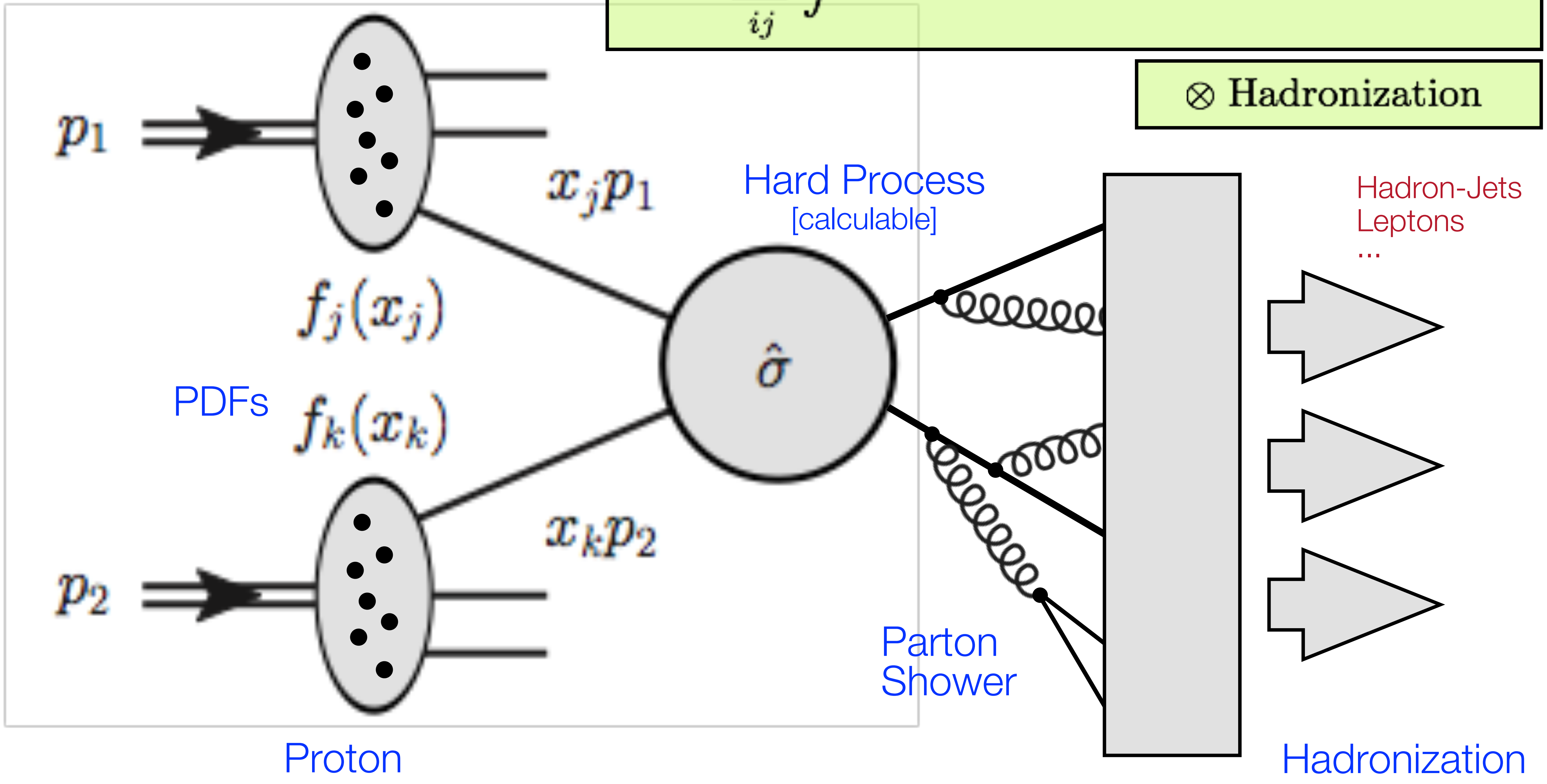

Proton

Hard Process
[calculable]

Hadron-Jets
Leptons
...

PDFs

Parton
Shower

Proton

Hadronization
[phenomenological]

[see later]

Particle Production @ LHC

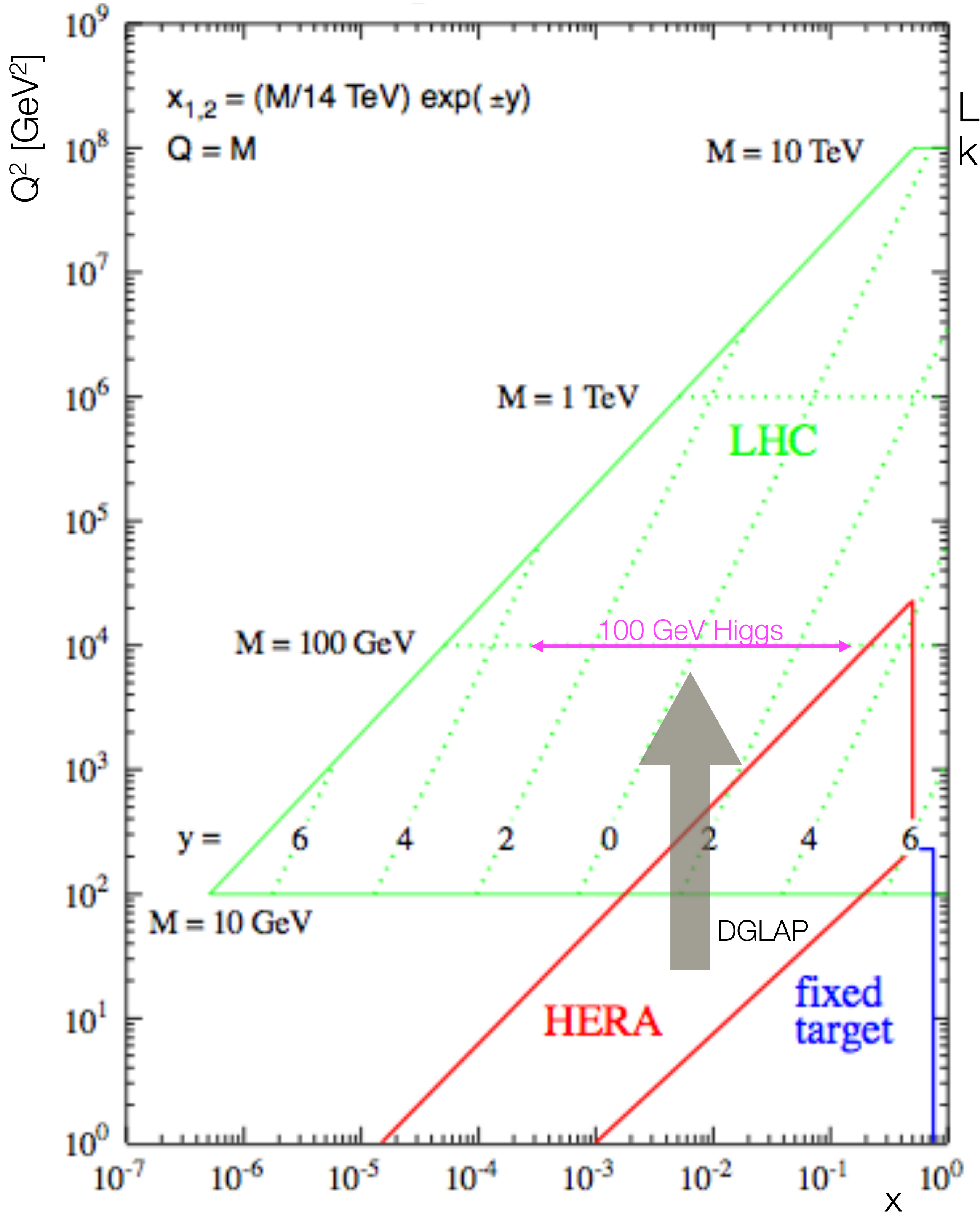

LHC parton kinematics

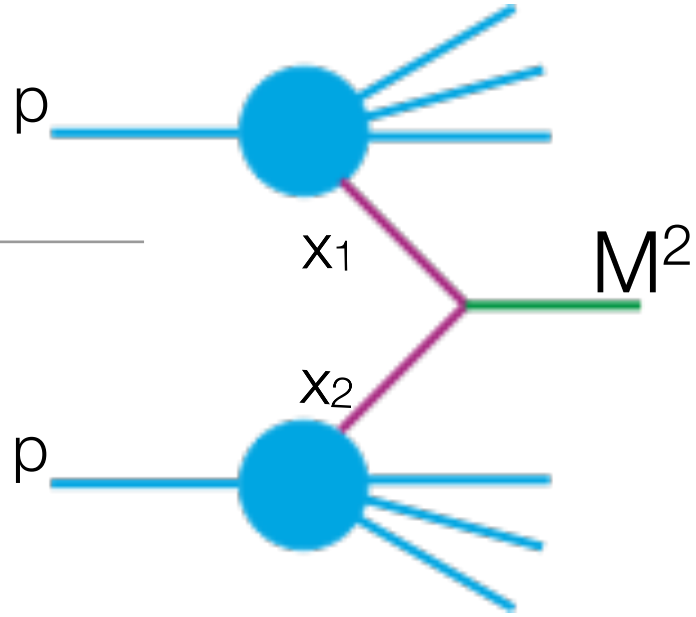

pp ➛ X_M + remnants

X_M: particle with mass M
e.g. Higgs

$M^2 = x_1 x_2 \cdot s$

i.e. to produce a particle with mass M
at LHC energies ($\sqrt{s}$ = 14 TeV)

$\langle x \rangle = \sqrt{x_1 x_2} = M/\sqrt{s}$

[$x_1 = x_2$: mid-rapidity]

LHC needs:

Knowledge of parton densities
Extrapolation over orders of magnitudes

Higgs Cross Section

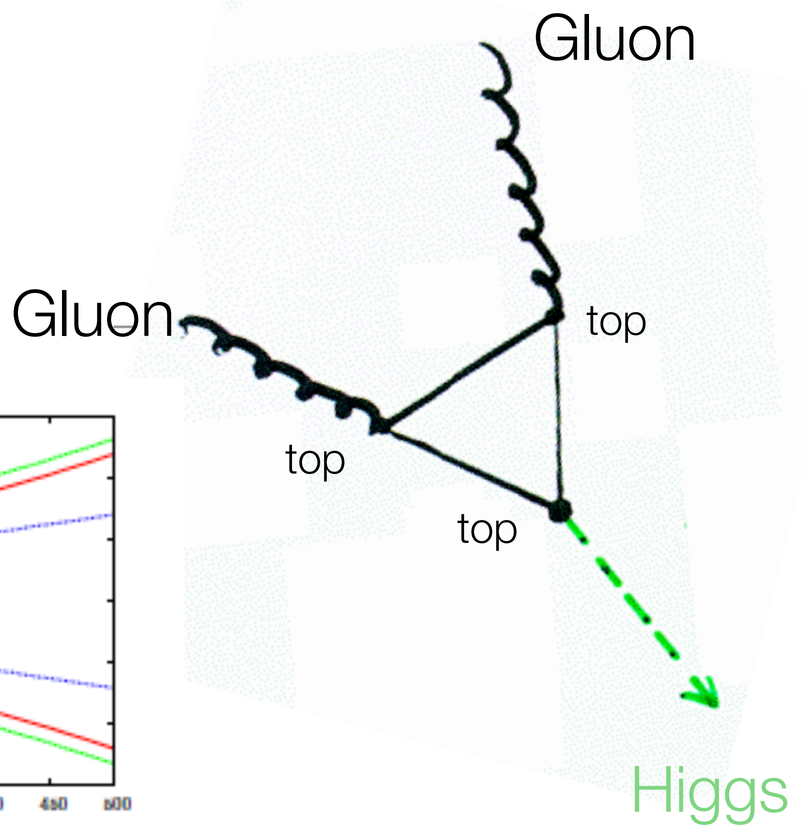

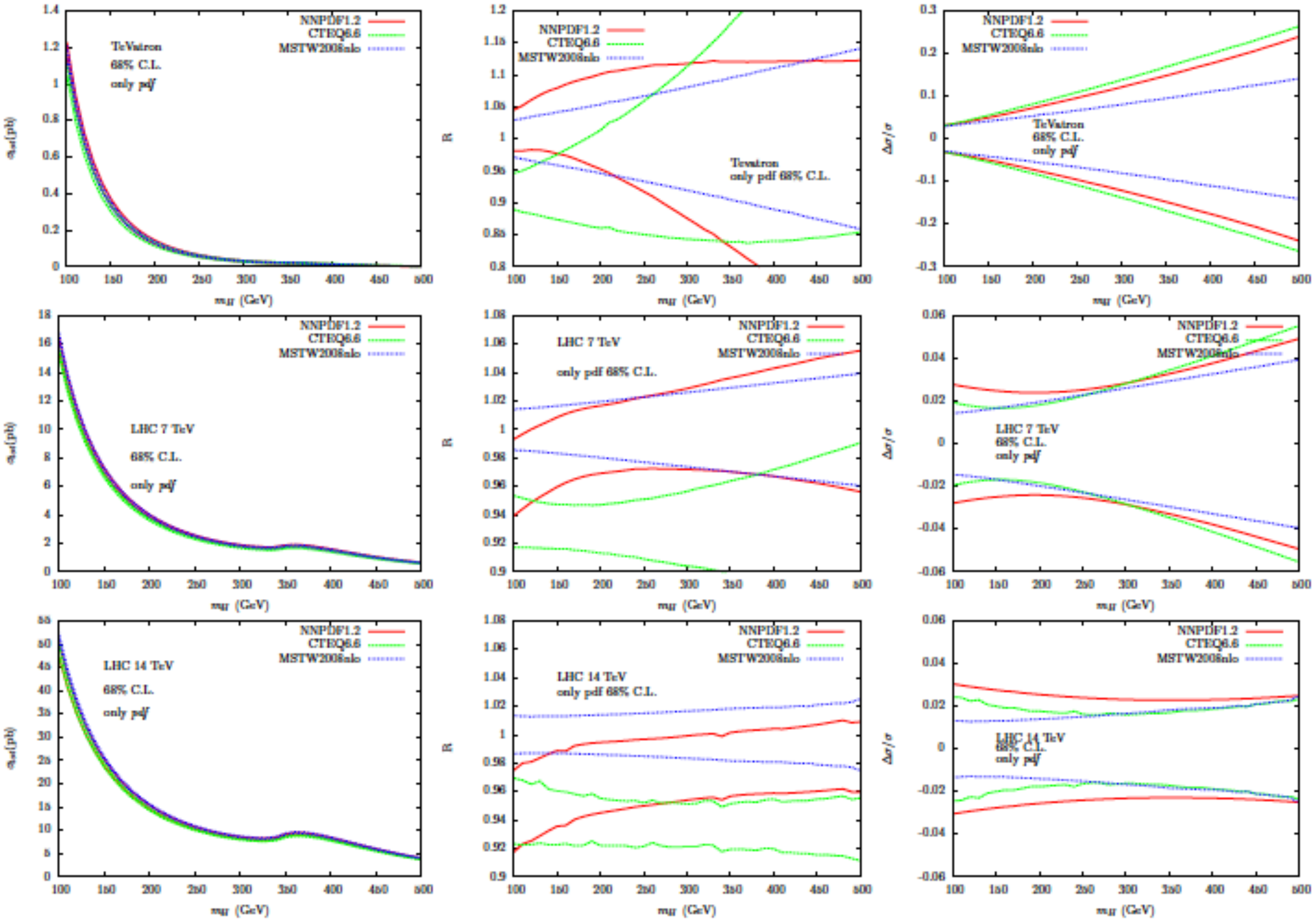

The left column shows absolute results,
the central column results normalized to the MSTW08 result, and the right column results
normalized to each group's central result.

10 – 20 % PDF uncertainty

m_H

Relative Uncertainty [compared to CTEQ 6.1M]

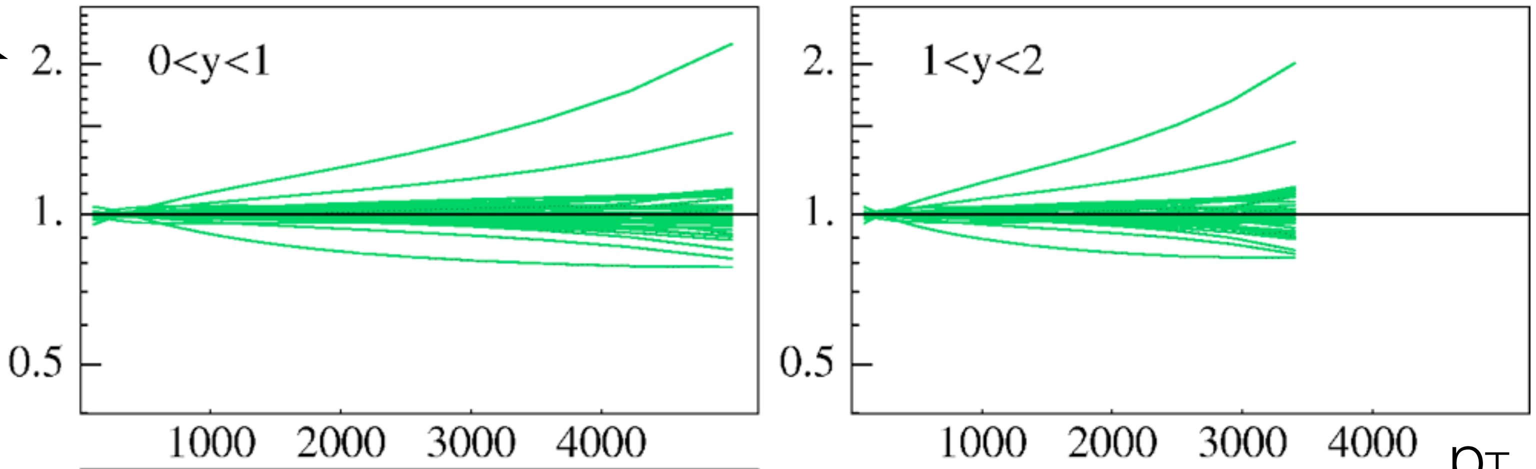

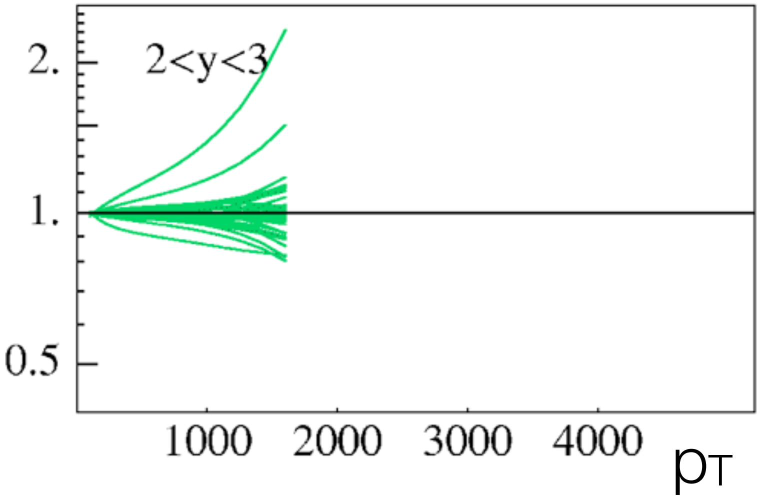

Inclusive Jet Cross Section @ LHC

[D.Stump et al., JHEP 10 (2003) 046]

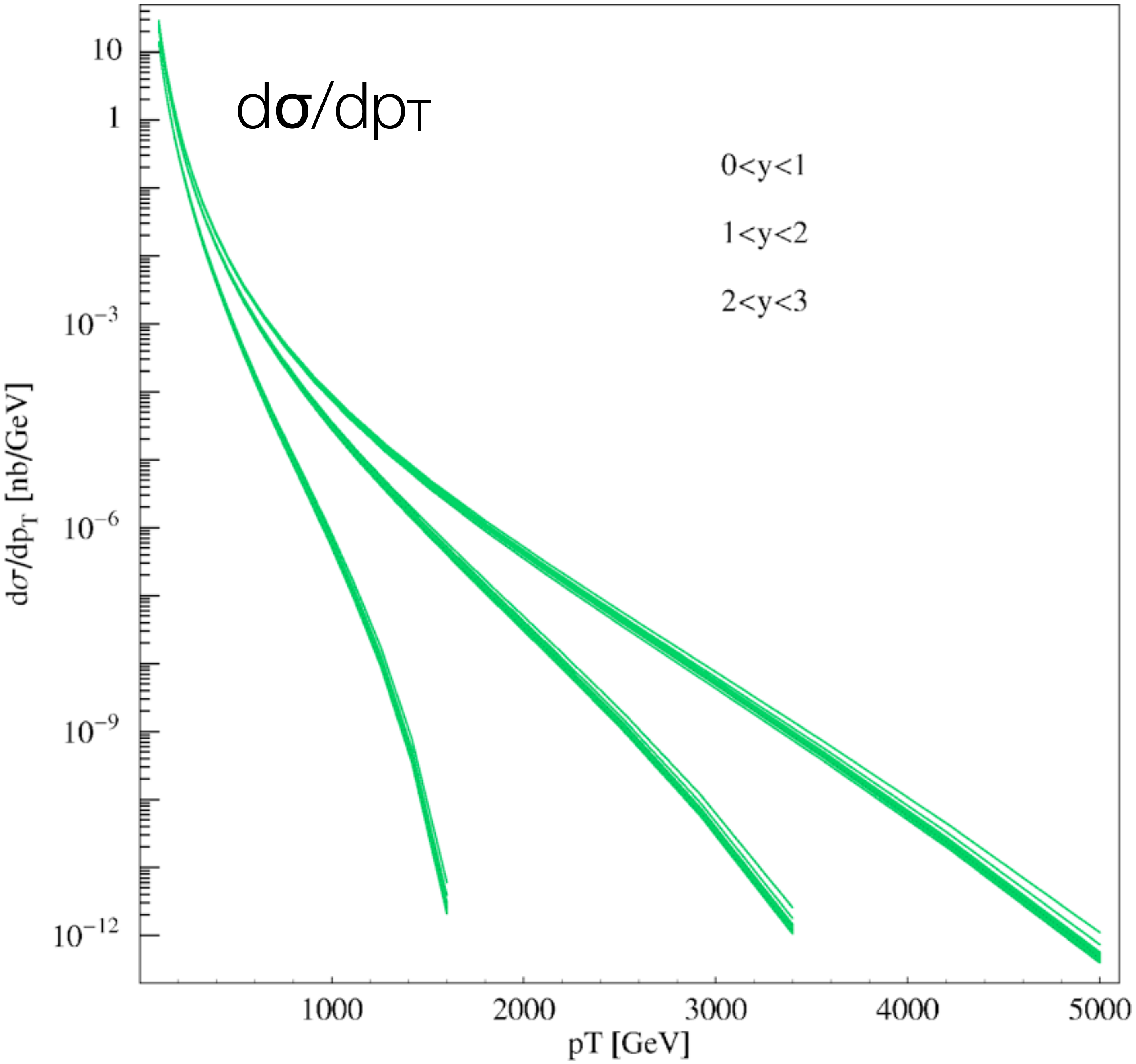

Mid-rapidity:
100 % uncertainty
@ E_T ~ 5 TeV

Forw. jets:
100 % uncertainty
@ E_T ~ 2 TeV

Inclusive Jet-Cross Section

Inclusive

Jet cross-section

[~Tevatron x 100]

- Restricted to 17 nb^{-1}
  [no pile-up contamination];
- $p_T > 60$ GeV and $|y| < 2.8$

Measured jets corrected to particle level using Monte Carlo

- Experimental uncertainties dominated by JES

Good data-MC agreement over 5 orders of magnitude!

[Important for Searches]

Inclusive Jet Cross Section

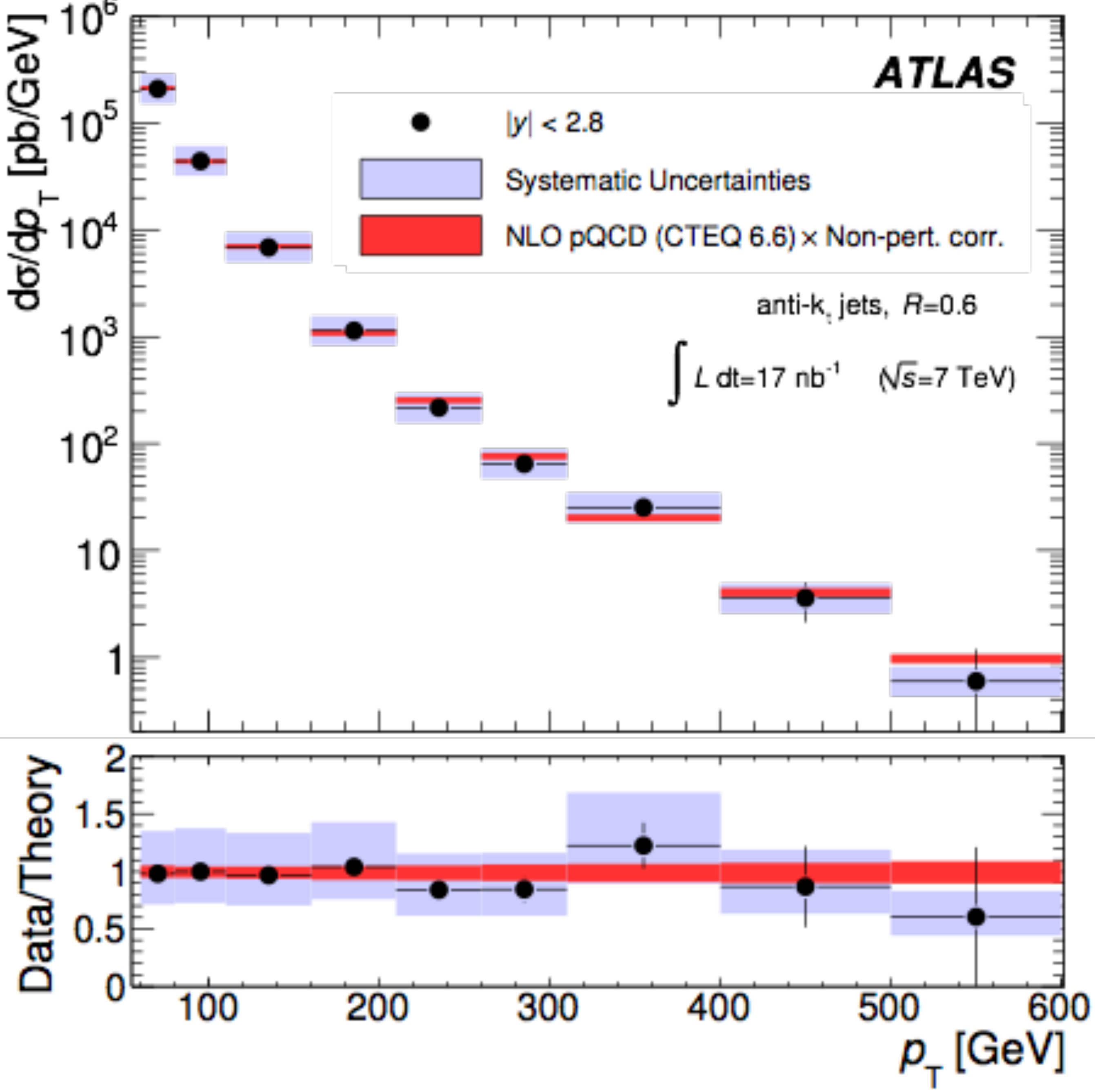

W and Z Production @ LHC

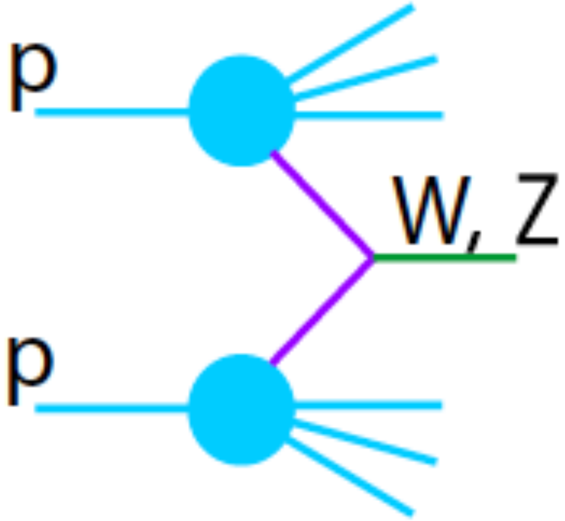

pp → W + X
pp → Z + X

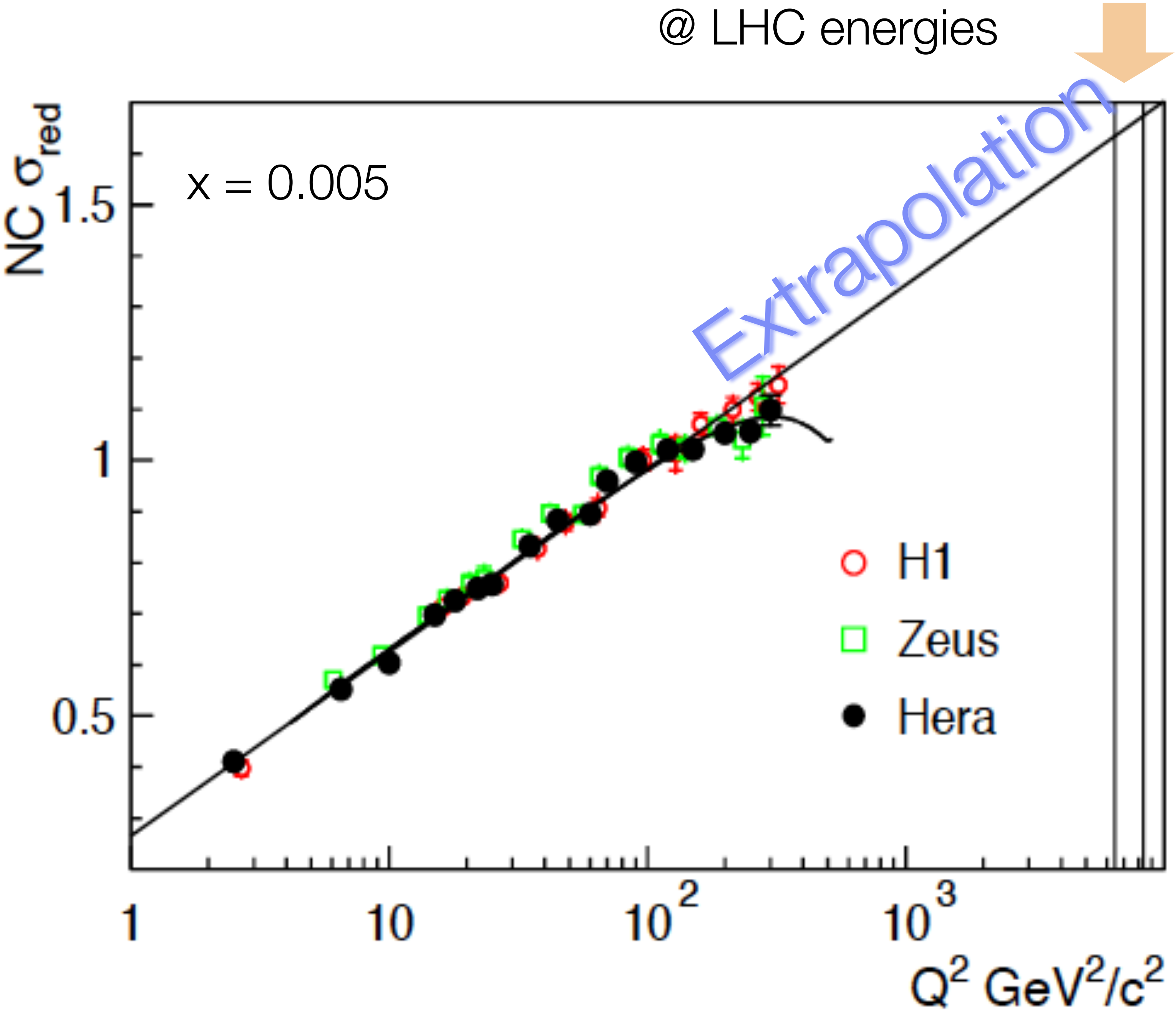

Q^2 for W/Z production
@ LHC energies

Considered
as luminosity monitor

Vector Boson Production

Direct γ-production:

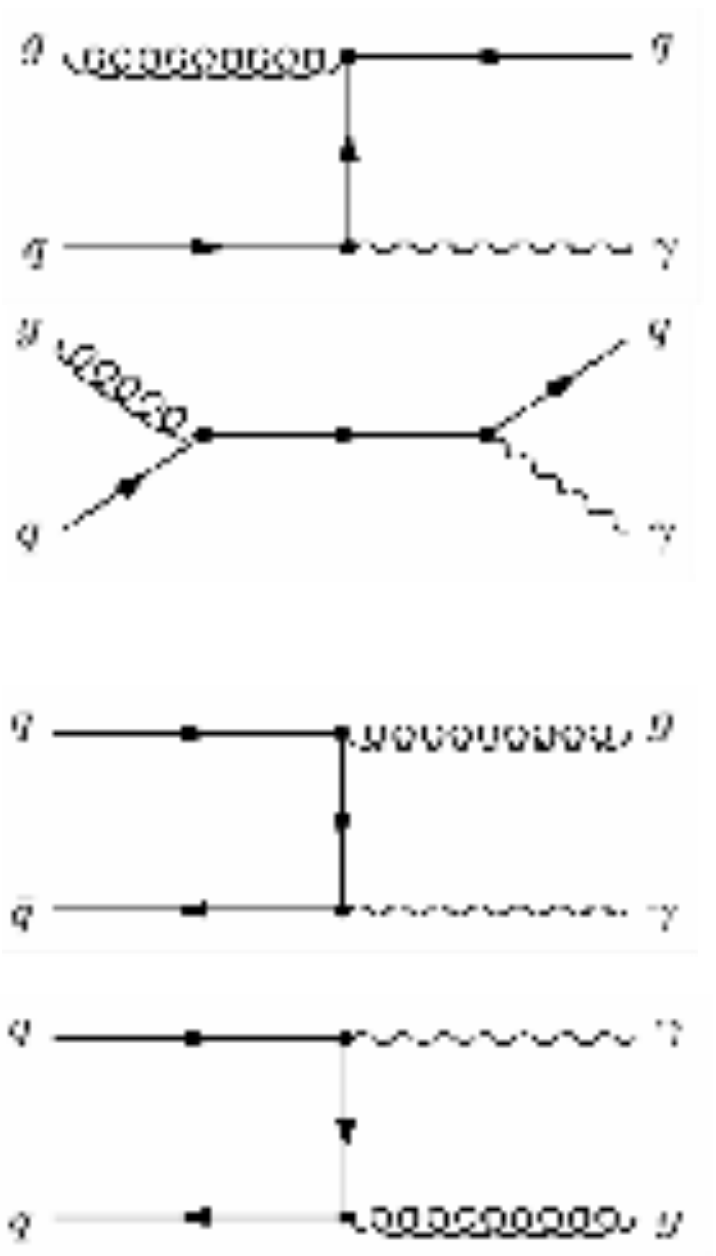

Singel W/Z production:

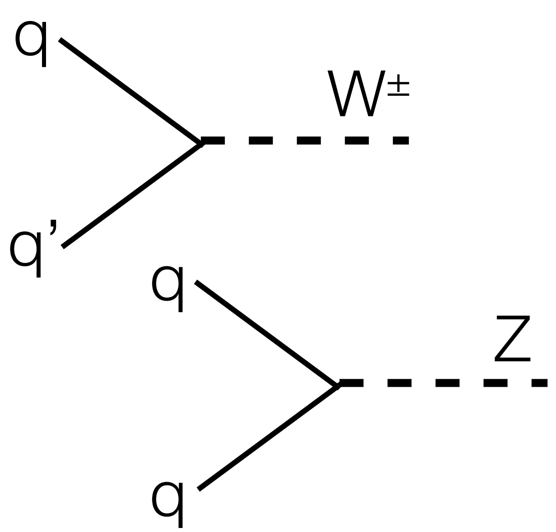

W production: $\begin{cases} u\bar{d} \to W^+ \\ d\bar{u} \to W^- \end{cases}$

(main contributions)

Z production: $\begin{cases} u\bar{u} \to Z \\ d\bar{d} \to Z \end{cases}$

(main contributions)

- At LHC energies these processes take place at low values of Bjorken-x
- Only sea quarks and gluons are involved
- At EW scales sea is driven by the gluon, i.e. x-sections dominated by gluon uncertainty

➥ Constraints on sea and gluon distributions

Effect on PDFs of LHC W data

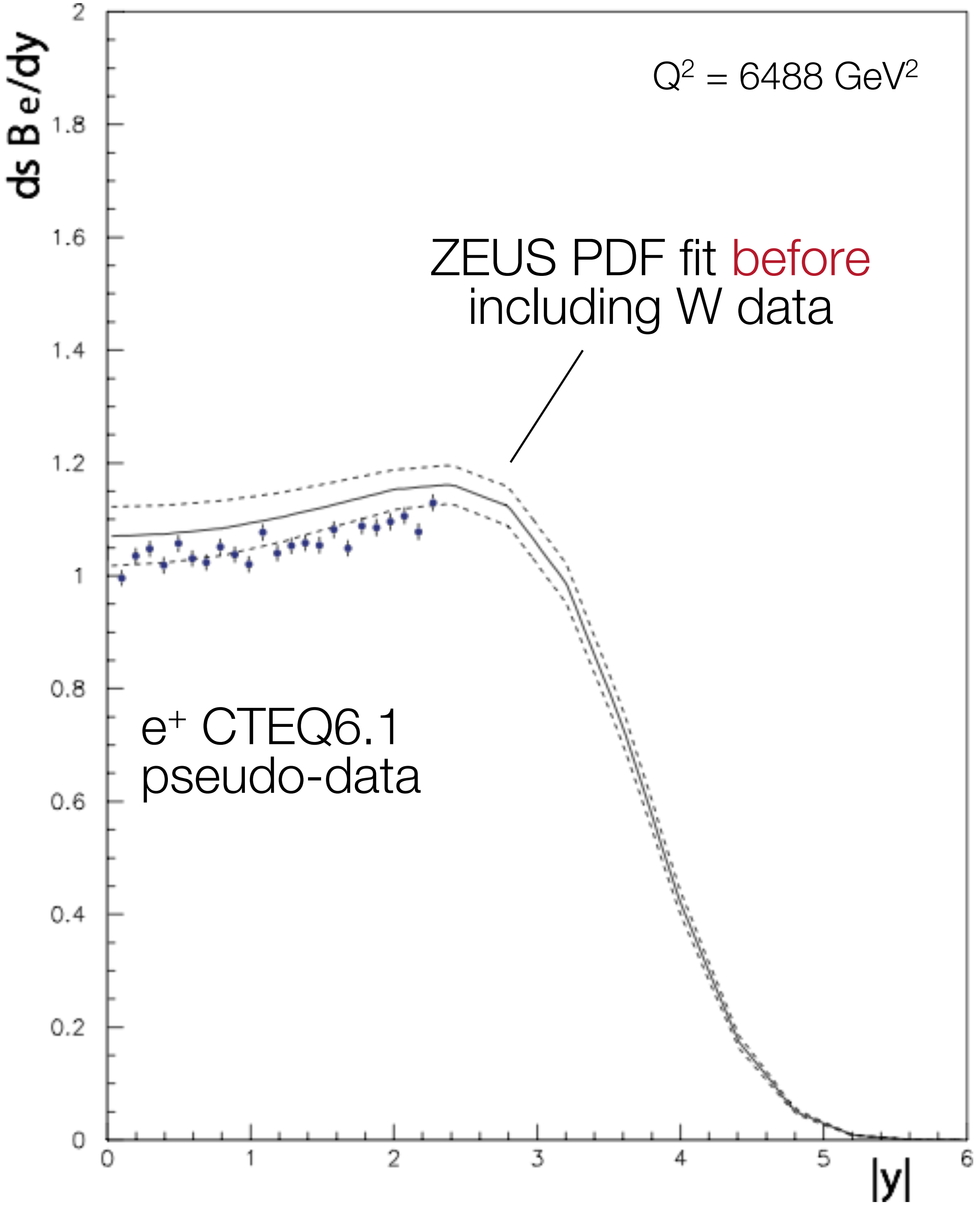

ZEUS PDF fit before including W data

e^+ CTEQ6.1 pseudo-data

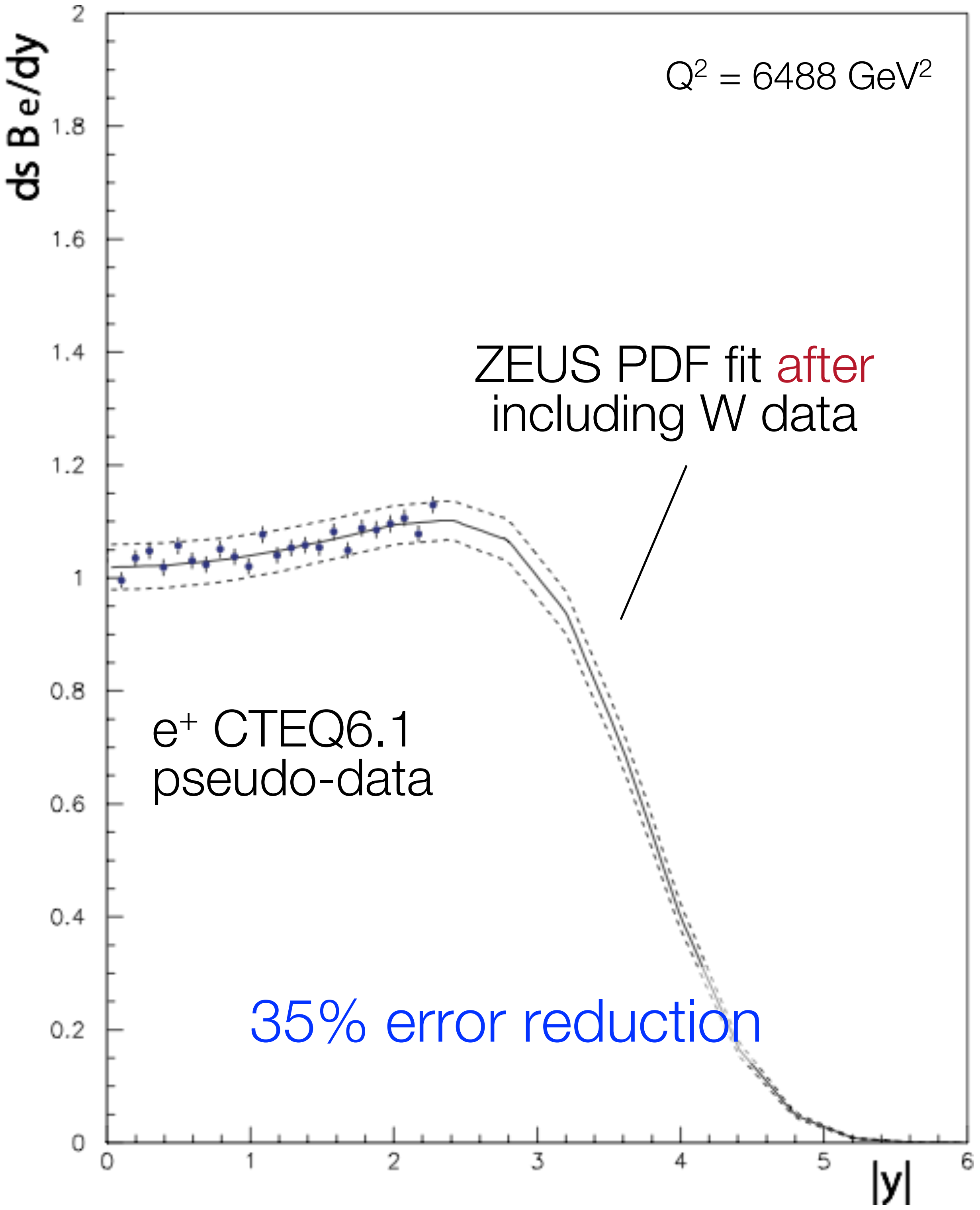

ZEUS PDF fit after including W data

e^+ CTEQ6.1 pseudo-data

35% error reduction